Jurnal Teknik Sipil & Perencanaan 26 (1) (2024) p 1-4

UNNES JOURNALS

JURNAL TEKNIK SIPIL & PERENCANAAN

http://journal.unnes.ac.id/nju/index.php/jtsp/index

# Analysis and Monitoring of Land Subsidence Phenomena in Tambak Lorok, Semarang City Using the In-sar Method

Fadhila Tiara Avrilia[1], Rini Kusumawardani[2]

[1,2,3,4] Department of Civil Engineering, Faculty of Engineering, Semarang State University, Semarang, Indonesia.

[a)] Corresponding author: rini.kusumawardani@mail.unnes.ac.id

**Abstract.** Rapid urbanization and infrastructure expansion in Semarang, particularly in the northern coastal areas, have led to significant land subsidence. Tambak Lorok, located in Tanjung Mas Sub-district, is among the affected areas, with key contributing factors including soft young alluvial soils, excessive groundwater extraction, infrastructure loads, coastal sediment dynamics, and tidal fluctuations. To understand the patterns and rates of land subsidence, this study employs the *Interferometric Synthetic Aperture Radar* (InSAR) method using the *Sentinel Application Platform* (SNAP).
The methodology involves the analysis of Sentinel-1A satellite imagery (2020–2024), *Digital Elevation Model* (DEM) mapping, and examination of changes in watershed (DAS) areas. Additional data were gathered through local community interviews and analysis of Google Maps and DEM data from 2018–2024. Long-term InSAR monitoring reveals that certain areas in North Semarang's coastal zone are subsidining at rates between -0.16 to -0.23 meters per year. Data validation was conducted through triangulation to ensure result accuracy.
These findings highlight the need for more effective mitigation strategies, such as stricter groundwater management, adaptive infrastructure upgrades, and spatial planning that considers subsidence risks. Furthermore, remote sensing technology should be complemented with ground-based monitoring to ensure more accurate and data-driven mitigation strategies. The outcomes of this research are expected to serve as a basis for disaster mitigation and sustainable coastal spatial planning.

Keywords: *Land Subsidence, InSAR, Sentinel-1A, SNAP, Digital Elevation Model, Watershed (DAS), Tambak Lorok, Semarang City.*

## INTRODUCTION

*Land subsidence* refers to the sinking of the Earth's surface due to factors such as soil consolidation and groundwater extraction. This phenomenon has garnered global concern as it contributes to tidal flooding, as observed in Tambak Lorok, Semarang. The area contains soft alluvial soil that accelerates subsidence by over 10 cm per year, exacerbated by tidal effects and watershed changes.
Subsidence in Tambak Lorok creates basins that disrupt water flow and elevate flood risks. Other contributing factors include land-use changes and infrastructure development. To monitor this phenomenon, InSAR techniques utilizing Sentinel-1A satellite data (2019–2024) were applied. This radar-based analysis provides an accurate depiction of subsidence patterns, which can guide mitigation and spatial planning efforts.

## EXPERIMENTAL

### Study Area

The study site is Tambak Lorok in Tanjung Mas Sub-district, located in northern Semarang. The region's geomorphology is significantly influenced by human activities, including groundwater extraction, infrastructure development, and coastal economic activities. As a result, tidal flooding is frequent in this area.


**FIGURE 1.** Research location review area, Tambak Lorok Semarang City

## Geological Conditions

Semarang's geology varies widely. Northern areas like Tambak Lorok are dominated by alluvial soils formed from silt, sand, and gravel deposits caused by tidal and river flows. Soil types include heavy clay grumusol (Tugu), light-textured regosol (Genuk), and gray alluvial soils (Pedurungan). In hilly areas (Ngaliyan, Tembalang, Banyumanik, Gunung Pati), brown and reddish-brown latosols dominate, while dark brown Mediterranean soils are common in the rain-heavy southern areas. Semarang's topography comprises a northern lowland (ideal for housing and flat agriculture), a central urban area, and southern hills.

## Interview Assessment

To investigate subsidence, field evaluations and community interviews were conducted. Visual inspections assessed damage to buildings and infrastructure, while interviews provided local perspectives on the phenomenon. Findings revealed structural cracks, road deformations, and drainage issues, along with socioeconomic impacts such as financial burdens and maintenance difficulties.

# METHOD

*Interferometric Synthetic Aperture Radar* (*InSAR*) measures Earth surface changes using radar wave phase differences between two or more satellite images, generating interferograms. This technique enables high-precision detection of elevation and land movement, down to millimeter scales. Though limited by inconsistencies, these are mitigated through time-series techniques like PSI-SBAS, SqueeSAR, and radar tomography. The open-source Sentinel Application Platform (SNAP) from the European Space Agency (ESA) was used to process SAR imagery and visualize displacement maps.

# RESULT AND DISCUSSION

Subsidence in North Semarang, especially coastal zones, is driven by excessive groundwater use and development, increasing the risk of flooding during high tides and storms. InSAR analysis from 2020–2024 shows subsidence rates in Tambak Lorok ranging from -0.075 to -0.23 m/year. These findings are visualized using color scales to indicate elevation changes.

(a)

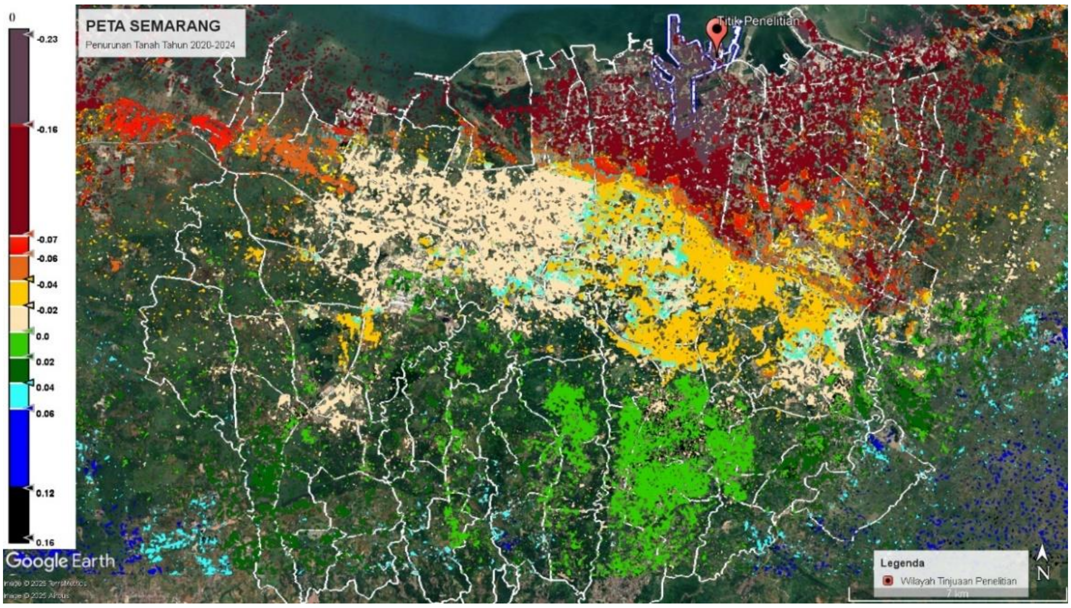


(b)

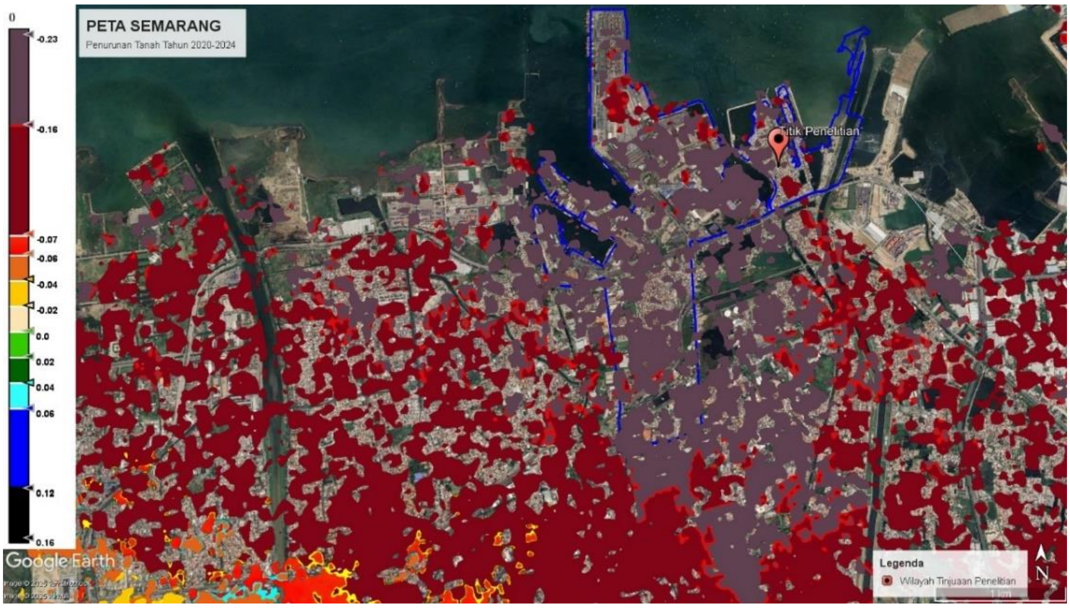


**FIGURE 2.** (a) & (b) The results of the analysis of the spread of the land subsidence phenomenon in the northern part of Semarang City area for 4 years of observation (2020-2024) in meters

Areas in red (coastal zones) indicate the highest subsidence (-0.23 m/year), primarily in densely urbanized regions influenced by soil compaction, groundwater exploitation, and infrastructure loads. This accelerates risks such as urban flooding, coastal erosion, and infrastructure damage. Subsidence may also alter watershed patterns by redirecting runoff, although causality requires further research. Additional contributing factors include sedimentation, erosion, and human activity. Survey and Sentinel-1A data suggest subsidence rates of 10–13 cm/year, gradually impacting infrastructure and communities.

Figures  depict building and infrastructure damage over time. By 2022, house entrances had sunken to ground level, prompting foundation renovations. By 2024, homes had been reconstructed with sturdier structures. Impacts include foundation risks, drainage issues, and aesthetic changes.

## CONCLUSION

The analysis indicates that subsidence rates in Tambak Lorok vary by geographic zone, with the highest occurring in the northern coastal area at -0.23 meters over four years. The lowland area shows moderate subsidence, while the southern region remains stable. Residents report floors and roads sinking below water levels, necessitating regular land filling. Tidal flooding has decreased due to seawalls, but rain-induced floods persist. Other impacts include reduced quality of life, financial losses, and psychological stress due to unstable infrastructure.

### Disclaimer

This article is intended to provide general insights into civil engineering and is not a substitute for professional advice. The authors and publisher are not liable for any errors, omissions, or consequences arising from the use of this information. Professional consultation is recommended before applying the concepts discussed

### Data and Material Availability

This article contains data and materials sourced from reputable references. However, the authors do not guarantee the accuracy, completeness, or timeliness of the presented information. Readers assume responsibility for their use of this data. Further inquiries can be directed to the authors.

## ACKNOWLEDGMENTS

I would like to express my deepest gratitude to the Soil Mechanics Laboratory of Universitas Negeri Semarang for the knowledge and support provided during the preparation of this article. The insights and guidance offered were invaluable in helping me understand and develop the topic discussed, serving as a valuable foundation for both my academic and professional journey, as well as that of my peers. Once again, thank you for your unwavering assistance and dedication.

I would also like to thank my friends for their support, thoughtful discussions, and encouragement throughout the completion of this article. The camaraderie and collaboration we shared have been truly meaningful in this academic endeavor.

## REFERENCE

[1] A., Ilfiyaningrum, A., Kusumawardani, R., Savanti, F., Setyohadi Kuswarna Putra, B., Aida, N., Biela Simanungkalit, R., Ayu Praditya Ning Putri, G., & Inas Saraswati, Z., Scientific Application of Technology. (n.d.) (2023). APTEK JOURNAL Estimation of Land Subsidence Using the Differential Interferometry Synthetic Aperture Radar (Dinsar) Method in Pantura, Semarang City. https://doi.org/10.30606/aptek.v16i1.2193

[2] American Association of State Highway and Transportation Officials. (1967).*AASHTO standard specifications for highway materials and methods of sampling and testing* (8th ed.). American Association of State Highway and Transportation Officials.

[3] Baillie, I. C. (2001b). Soil Survey Staff 1999, Soil Taxonomy. Soil Use and Management,

[4] 7(1), 57–60. https://doi.org/10.1111/j.1475-2743.2001.tb00008.x

[5] Budianto, E. (2016). Land subsidence on the north coast of Java, Village Bandarharjo and its surroundings, Semarang City, Central Java. *Journal of Geoscience*.

[6] SINGLE. (2015/2012). Sentinel-1. European Space Agency.

[7] Galloway, D. L., Jones, D. R., & Ingebritsen, S. (1999). Land subsidence in the United States. *U.S. Geological Survey Circular.* https://doi.org/10.3133/cir1182

[8] Ministry of Public Works and Public Housing (PUPR). (2021). *Geotech Guide-nik: The formation process and basic properties of soft soils*. Retrieved from https://binamarga.pu.go.id

[9] Lisa N. I., at al, "Analysis of Land Decline in Semarang City Survey Method Gnss Year 2019", Undip Geodesy Journal, Volume 9, Number 2, Year 2020, (ISSN :2337-845X)

[10] Pramono, I. B. (2021). Nature-based solutions for integrating flood and land subsidence: A case study in Jakarta and Semarang. *IOP Conference Series Earth and Environmental Science*, *874*(1), 012001.https://doi.org/10.1088/1755-1315/874/1/012001

[11] Pujiastuti, R., Suripin, S., & Syafrudin, S. (2016). The Effect of Land Subsidence on Gena-only Flood and Rob in East Semarang. *SIPIL TECHNICAL COMMUNICATION MEDIA, 21*(1), 1. https://doi.org/10.14710/mkts.v21i1.11225

Jurnal Teknik Sipil & Perencanaan 26 (1) (2024) p 5-10

JURNAL TEKNIK SIPIL & PERENCANAAN

http://journal.unnes.ac.id/nju/index.php/jtsp/index

# Feasibility Study on the Use of Fly Ash and Bottom Ash as Aggregate Substitutes in the Subbase Layer of Road Pavement

M. Arief Firdaus[a)], Rini Kusumawardani[2], Nirima Ramadhani[3], Zahra Aulia Putri[4]

[1,2,3,4] Civil Engineering Study Program, Semarang State University, Postal Code 50229

[a)] Corresponding author: marieffirdaus@students.unnes.ac.id

**Abstract.** This study used fly ash and bottom ash (FABA) waste as a substitute for aggregate in the *road subbase* layer. The initial mixture included FABA with a depth of 1 meter and 7 meters without mixing other materials. This mixture is differentiated into two variations with a ratio of variation I (70:30) and variation II (70:30), each fermented for 14 days. The test results showed that the FABA material did not meet the specification of SNI 6388:2015 for class B foundation layers, with a maximum immersion CBR value of 25.32% in variation I and 18.99% in variation II. This study evaluates the feasibility of using FABA as an aggregate substitute material in the *subbase* layer of road pavement. From the results obtained, FABA material has the potential to be used in *subbase construction*. Still, adding other materials such as cement or lime is necessary to increase the carrying capacity and meet the set specifications.

Keywords: *Bottom ash*, *fly ash*, alternative materials, *subbase*

## INTRODUCTION

Along with the increasing demand for electricity in Indonesia's manufacturing industry sector, the use of coal as the primary fuel in coal-fired power plants also continues to grow. The coal that is burned produces electrical energy but also leaves residues in the form of *fly ash* (flying ash) and *bottom ash* (base ash). The demand for coal for power plants has increased significantly from 56 million tons in 2006 to 123.2 million tons in 2025, which is expected to produce around 11.38 million tons of FABA (UGRG FT UGM, 2022).

Government Regulation Number 101 of 2014 concerning the Management of Hazardous and Toxic Waste (B3). FABA is categorized as B3 waste because the content of FABA waste contains heavy metal oxides that will pollute the environment. However, FABA is no longer included in B3 waste by Government Regulation (PP) Number 22 of 2021 as non-B3 waste. One way to determine the concentration of pollutants in FABA is by the *toxicity characteristic leaching procedure* (TCLP) test.

One of the power plant managers in Indonesia is the Tanjung Jati B Jepara Power Plant. The capacity of this coal-fired power plant reaches 4 x 710 MW Gross or 4 x 660 MW Nett, which accounts for around 12% of Java-Bali electricity needs (PLN, 2019). By-products of burning coal include *fly ash*, *bottom ash, and* flue gas desulfurization *(FGD) sludge*. About 80-90% of the combustion residue is fly ash, while the remaining 10-20% consists of base ash (Darwis & Hidayat, 2015).

*Fly ash* is a fine-grained product from coal combustion, derived from the minerals silicates, sulfates, sulfides, carbonates, and oxides found in coal (ASTM C.618). Meanwhile, *bottom ash* is a coarser and heavier residue, which settles at the bottom of the combustion furnace after the combustion process is complete (Hanafie, 2023). FABA has a very varied material composition, depending on the source and content of the coal used in combustion. Nonetheless, this material mainly contains major inorganic compounds such as silicon dioxide ($SiO_2$) and calcium oxide (CaO).

FABA material can be used as an alternative material for mixed materials that make up road pavement layers, such as the upper foundation layer (*roadbase*), the lower foundation layer (*subbase*), and the base soil layer (*subgrade*). The utilization of FABA helps reduce waste and supports sustainability by reducing dependence on natural materials. This study evaluates the feasibility of using FABA as the primary material in constructing *road* pavement subbase layers by considering technical, economic, and environmental aspects.

## LITERATURE REVIEW

### 1.1 Bending Pavement

Flexible pavement is pavement that uses asphalt as a binding material. In general, flexible pavement construction consists of four main layers, namely the *surface course*, the upper foundation layer (*base course*), the lower foundation layer (*subbase course*), and the base layer (*subgrade*). Based on the Road Pavement Design Manual No. 03/M/BM/2024 and SNI 6388:2015, the material used for the upper foundation layer (*base course*) is class A aggregate, while the lower foundation layer (*subbase course*) uses class B aggregate.

### 1.2 Foundation Layer

According to Suprapto (2004), the foundation layer in flexible pavement is part of the road pavement structure that distributes the vehicle load evenly from the surface layer to the layer below it, thereby reducing the direct pressure on the subgrade soil. Determination of materials in the lower foundation layer (subbase) requires sieve requirements and properties of foundation layers for class A, class B, and class S by SNI 6388:2015, as shown in Table 1 and Table 2.

**TABLE 1.** Sieve size requirements

| Ukuran ayakan | | Persen berat yang lolos (%) | | |
|---|---|---|---|---|
| | | Kelas A | Kelas B | Kelas S |
| 2" | 50 mm | - | 100 | - |
| 1 1/2" | 37,5 mm | 100 | 88 - 95 | 100 |
| 1" | 25,0 mm | 79 - 85 | 70 - 85 | 77 - 89 |
| 3/8" | 9,50 mm | 44 - 58 | 30 - 65 | 41 - 66 |
| No. 4 | 4,75 mm | 29 - 44 | 25 - 55 | 26 - 54 |
| No. 10 | 2,0 mm | 17 - 30 | 15 - 40 | 15 - 42 |
| No. 40 | 0,425 mm | 7 -17 | 8 - 20 | 7 - 26 |
| NO. 200 | 0,075 mm | 2 -8 | 2 - 8 | 4 - 16 |

**TABLE 2.** Condition properties of foundation layer, lower foundation layer, and road shoulder

| Uraian persyaratan | Standar | Nilai | | |
|---|---|---|---|---|
| | | Kelas A | Kelas B | Kelas S |
| Abrasi/*Los Angeles* | SNI 2417:2008 | Maks. 40% | Maks. 40% | Maks. 40% |
| Butiran pecah, tertahan ayakan No. 3/8 atau 9,5 mm | SNI 7619:2012 | 95/90[1] | 55/50[1] | 55/50[1] |
| Batas Cair (LL) | SNI 1967:2008 | Maks. 25% | Maks. 35% | Maks. 35% |
| Indeks Plastisitas (PI) | SNI 1966:2008 | Maks 6% | Maks. 10% | Maks. 10% |
| Hasil kali Indek Plastisitas dengan % Lolos Ayakan No.200 | - | Maks. 25% | - | - |
| Gumpalan lempung dan butiran - butiran mudah pecah | SNI 03-4141-1996 | Maks. 5% | Maks. 5% | Maks. 5% |
| CBR rendaman | SNI 1744:2012 | Min. 90% | Min. 60% | Min. 60% |
| Perbandingan % lolos ayakan No. 200 dan No. 40 | - | Maks. 2/3 | Maks. 2/3 | Maks. 2/3 |

## 1.3 *Fly Ash* and *Bottom Ash* (FABA)

Burning coal produces fly and bottom ash (FABA) waste. According to SNI 2460:2014, *fly ash* is a fine residue from burning coal in a steam power plant (PLTU). *Fly ash* has a high cement content and pozzolan properties, which allows it to react with quenched lime (Ca(OH)2) and water at room temperature, resulting in a solid compound that is insoluble in water.

*Bottom ash* is waste from coal burning at steam power plants (PLTU). The base ash falls to the bottom of the *boiler* and collects in the last *hopper*, also known as the final hopper. After being sprayed with water, the base ash is disposed of or used as an additive or alternative material on road pavement. *Bottom ash* is divided into dry *bottom ash* (*slag-tap boiler* and *cyclone boiler*) and *wet bottom ash* (*boiler slag*). The characteristics of *bottom ash* are very diverse because they depend on the type of coal used and the combustion system (Indriani Santoso et al., 2003).

# RESEARCH METHODS

The research was conducted using experimental methods in the laboratory to determine the feasibility of using FABA in constructing *road pavement subbases*. In this study, the SNI 6388:2015 specification and the 2018 Bina Marga general specification were used as a reference to determine the variation of FABA mixture in the lower foundation layer of class B using the soaked CBR test method.

## Materials used

1. FABA obtained from the Tanjung Jati B Jepara PLTU in Kembang District, Sekuping, Tubanan, Jepara Regency, Central Java.


**FIGURE 1.** FABA 1 meter deep


**FIGURE 2.** FABA 7 meters deep

2. Clean water

## Equipment used

1. CBR Laboratory Testing Machine
2. Los Angeles *abrasion testing machine* with steel balls
3. Proctor *compaction machine*
4. Drying oven
5. Soaking tub
6. Scales
7. Test case
8. Other equipment

## FABA material testing

The tests that will be carried out to determine the characteristics and feasibility of FABA materials in the construction of the lower foundation layer (*subbase*) are as follows:

1. Specific gravity testing based on SNI 03-1970-2008
2. Permeability test based on SNI 2435:2008
3. Screening analysis testing based on SNI 3423:2008
4. Aggregate wear testing with the Los Angeles abrasion machine based on SNI 2417:2008
5. Testing of 3/8 inch aggregate broken grain percentage based on SNI 7619:2012
6. Testing of clay and grain lumps – easily broken grains based on 03-4141-1996
7. Atterberg limit *testing* based on SNI 1966:2008
8. Density testing or compaction based on SNI 1742:2008
9. Immersion CBR testing based on SNI 1744:2008

### Determination of FABA mixture variations

Based on this study, two mixed variations were used, namely variation I, 70% FABA, 1 meter, and 30% FABA, 7 meters. For variation II, the same as variation I, but in fermentation for 14 days.

# RESULTS AND DISCUSSION

## FABA material *properties* test results

Based on the tests carried out, a recapitulation can be made, which is presented in the following table.

**TABLE 3.** Recapitulation of *FABA* Properties Test Results

| Parameter | FABA 1 | FABA 7 |
|---|---|---|
| Warna | Abu tua | Hitam gelap |
| Berat jenis, (gr/cm$^3$) | 2,28 | 2,30 |
| Permeabilitas, (cm/det) | $5{,}19\times10^{-4}$ | $3{,}36\times10^{-4}$ |
| Kadar air optimum, (%) | 17,94 | 18,68 |
| Kepadatan kering, (gr/cm$^3$) | 0,85 | 0,80 |
| Abrasi *Los Angeles*, (% lolos) | 73,24 | 77,77 |
| Batas cair, (%) | 31,85 | 29,87 |
| Plastisitas | Non plastis | Non plastis |
| Cu/*Uniformity coefficient* | 3,11 | 5,12 |
| Cc/*Coefficient of curvature* | 1,10 | 1,02 |

Table 3 shows that FABA 1 has properties more similar to *fly ash* than *bottom ash* due to its lighter color, lower specific gravity value than FABA 7, and the Cu value in FABA 1, including sand that has a range of 1 – 3, indicates that the particles have a good or more uniform gradation. In contrast, FABA 7 tends to be more similar to *bottom ash* because of its darker color, higher specific gravity values, and higher Cu values than FABA 1, indicating that the particles are often larger and less uniform.

## FABA Eligibility Test Results

Based on the tests carried out, a recapitulation can be made, which is presented in the following table.

**TABLE 4.** Feasibility Test Results of Class B Foundation Layer on Variation I

| Uraian persyaratan | Kelas B | Variasi I 70% FABA 1 - 30% FABA 7 | Memenuhi/ tidak |
|---|---|---|---|
| Abrasi/*Los Angeles* (SNI 2417:2008) | 0 - 40% | 52,17% | TM |
| Butiran pecah, tertahan ayakan No. 3/8 (SNI 7619:2012) | 55/50[1] | 77,74%/73,41%[1] | TM |
| Batas Cair (SNI 1967:2008) | 0 - 35% | 31,23% | M |
| Indeks Plastisitas (SNI 1966:2008) | 0 - 10% | Non-plastis | TM |
| Hasil kali Indeks Plastisitas dengan % Lolos Ayakan No.200 | - | - | TM |
| Gumpalan lempung dan butiran - butiran mudah pecah (SNI 4141:2015) | 0 - 5% | 10,20% | TM |
| CBR rendaman (SNI 1744:2012) | Min. 60% | 25,32% | TM |
| Perbandingan % lolos ayakan No. 200 dan No. 40 | Maks. 2/3 | 0,56 | M |

**TABLE 5.** Results of the Class B Foundation Layer Feasibility Test in Variation II

| Uraian persyaratan | Kelas B | Variasi II 70% FABA 1 - 30% FABA 7 Peram 14 hari | Memenuhi/ tidak |
|---|---|---|---|
| Abrasi/*Los Angeles* (SNI 2417:2008) | 0 - 40% | 52,17% | TM |
| Butiran pecah, tertahan ayakan No. 3/8 (SNI 7619:2012) | 55/50[1] | 77,74%/73,41%[1] | TM |
| Batas Cair (SNI 1967:2008) | 0 - 35% | 31,23% | M |
| Indeks Plastisitas (SNI 1966:2008) | 0 - 10% | Non-plastis | TM |
| Hasil kali Indeks Plastisitas dengan % Lolos Ayakan No.200 | - | - | TM |
| Gumpalan lempung dan butiran - butiran mudah pecah (SNI 4141:2015) | 0 - 5% | 10,20% | TM |
| CBR rendaman (SNI 1744:2012) | Min. 60% | 18,99% | TM |
| Perbandingan % lolos ayakan No. 200 dan No. 40 | Maks. 2/3 | 0,56 | M |

FABA material does not meet the specifications of SNI 6388:2015, so it is not recommended to use it as the primary aggregate material for grade B aggregate foundation layers. However, some parameters meet the requirements of SNI 6388:2015, such as liquid limit (LL) tests with a value range of 0 – 35%. It is therefore recommended that FABA material be added with other materials such as cement or lime, as this can increase the carrying capacity of the material and change some of its properties.

## CONCLUSION

From the results of the feasibility study on the use of *fly ash* and *bottom ash* (FABA) in construction *Subbase* of road pavement can be concluded as follows:

1. The effect of FABA mixture variation as the primary material in the construction of the lower foundation layer of class B, which has the potential to increase the bearing capacity of *the subbase layer* with the CBR value of immersion without mixing with other materials, a maximum result of 25.32% was obtained in variation I of a mixture of 70% FABA 1 and 30% FABA 7 without marinating.
2. FABA material that was given a curing treatment in variation II had a lower CBR value of immersion than in the non-fermentation condition, with a value of 18.99%.
3. The feasibility of FABA materials in the construction of the lower foundation layer (*subbase*) of the two variations does not meet the requirements of specification 6388:2015 and the general specification of Bina Marga 2018 because the minimum CBR value of immersion is 60%.

## REFERENCES


[1] Badan Standardisasi Nasional. (2015). *Standar Nasional Indonesia. Spesifikasi agregat untuk lapis fondasi, lapis fondasi bawah, dan bahu jalan*. SNI 6388:2015.

[2] Darwis, M., & Hidayat, R. (2015). *Karakteristik dan Pemanfaatan Abu Terbang dan Abu Dasar dari Pembakaran Batu Bara*. Jurnal Teknologi Lingkungan, 6(2), 123-130.

[3] Hanafie, M. (2023). *Karakteristik Fly Ash dan Bottom Ash dari Proses Pembakaran Batu Bara pada Pembangkit Listrik Tenaga Uap*. Jurnal Teknologi Lingkungan, 15(1), 45-60.

[4] Indriani Santoso, Patrick Patrick, Andarias Andarias, & Salil Kumar Roy. (2003). Pengaruh Penggunaan Bottom ash Terhadap Karakteristik Campuran Aspal Beton. *Civil Engineering Dimension, 5*, 75-81.

[5] UGRG FT UGM. (2022). *Limbah Padat Pembakaran Batubara: Potensi Sumber Daya Non-Konvensional di Masa Depan*. Tersedia di: https://ugrg.ft.ugm.ac.id/artikel/batubara- sebagai-sumber-energi-asal-jenis-dan-kegunaannya/ [Diakses 20 Maret 2025].

[6] Peraturan Pemerintah Republik Indonesia Nomor 101 Tahun 2014 tentang Pengelolaan Limbah Bahan Berbahaya dan Beracun. (2014). Ditetapkan pada 17 Oktober 2014. Tersedia di: https://peraturan.go.id/id/pp-no-101-tahun-2014 [Diakses 20 Maret 2025].

[7] Peraturan Pemerintah Republik Indonesia Nomor 22 Tahun 2021 tentang Penyelenggaraan Perlindungan dan Pengelolaan Lingkungan Hidup. (2021). Ditetapkan pada 2 Februari 2021. Tersedia di: https://jdih.maritim.go.id/id/peraturan-pemerintah-republik-indonesia-no-22- tahun-2021# [Diakses 20 Maret 2025].

[8] PT PLN (Persero). (2019, 10 Desember). *Melihat Lebih Dekat Pembangkit Besar PLTU Tanjung Jati B*. Tersedia di: https://web.pln.co.id/cms/media/siaran-pers/2019/12/melihat-lebih- dekat-pembangkit-besar-pltu-tanjung-jati-b/ [Diakses 20 Maret 2025].

Jurnal Teknik Sipil & Perencanaan 26 (1) (2024) p 11-14

JURNAL TEKNIK SIPIL & PERENCANAAN

http://journal.unnes.ac.id/nju/index.php/jtsp/index

# Interpretation of Subgrade Conditions Beneath Flexible and Rigid Pavement Layers Using Ground Penetrating Radar (GPR)

Detria Ardhila Kumala Sari[,a)] and Rini Kusumawardani[2]

[1,2]Undergraduate Civil Engineering Study Program, Department of Civil Engineering, Faculty of Engineering, Universitas Negeri Semarang

[a)] Corresponding author:

**Abstract.** Ground Penetrating Radar (GPR) is a device commonly utilized in non-destructive testing (NDT) applications. Its principal advantage lies in its non-invasive nature, allowing for subsurface exploration without causing damage to existing structures or the surrounding environment. Due to this characteristic, GPR has become a leading technology in subsurface investigation.

GPR is regarded as an optimal solution for rapidly and efficiently assessing subsurface conditions without inflicting damage on the pavement surface. In this research, GPR technology is employed to analyze the subgrade layers beneath flexible (asphalt) and rigid (concrete) pavements, with the objective of enhancing the effectiveness and sustainability of road maintenance strategies.

The data acquisition process is supported by the GAS XPC software for field data recording, while data processing is conducted using GPRSoft and GSSI RADAN 7. A comparison between raw and processed data reveals distinctions that facilitate a more in-depth analysis. Furthermore, discrepancies in data interpretation were observed between the outputs of GPRSoft and GSSI RADAN 7. These differences serve as valuable references for refining data analysis methods and improving the accuracy and reliability of future GPR-based investigations.

Keywords: Ground Penetrating Radar, flexible pavement, rigid pavement

## INTRODUCTION

Ground Penetrating Radar (GPR) is one of the most widely adopted near-surface geophysical methods for infrastructure imaging. A GPR system transmits radio wave signals into a structure and detects the echoes generated by changes in the material properties within that structure.

The GPR system consists of a transmitting antenna that emits electromagnetic signals and a receiving antenna that detects the reflected electromagnetic waves. The electromagnetic pulses emitted by the transmitting antenna into the ground are reflected, scattered, and transmitted by subsurface materials and are subsequently captured by the receiving antenna. These waves are reflected back to the surface by subsurface reflectors due to contrasts in electromagnetic properties, such as dielectric permittivity and electrical conductivity, relative to the surrounding environment.

Through this process, GPR records data representing the subsurface conditions. The recorded data can then be interpreted to produce a clearer depiction of soil structure, the presence of underground objects, or other geological characteristics.

GPR and geotechnical methods have been extensively applied in civil engineering, particularly for the inspection of pavement layers. In road assessment, a primary application is evaluating the variability of volumetric water content in the sub-base or subgrade, thereby enabling the monitoring of soil stability in the area.

In this study, the data acquisition process was supported by GAS XPC software for field data recording, while data processing was carried out using GPRSoft and GSSI RADAN 7.

## LITERATURE REVIEW

Electromagnetic waves are unique in that they can propagate through a vacuum without requiring a medium such as air or water. These waves consist of electric and magnetic field components that are perpendicular to each other and also perpendicular to the direction of wave propagation.

The behavior of electromagnetic waves is mathematically described by Maxwell's equations. Maxwell's equations consist of four field equations, each representing the relationship between the fields and their sources (i.e., charge or current distributions).

Maxwell's first equation states that a changing magnetic field can induce an electric field:

(1) $$\bar{\nabla} \times \bar{E} = -\frac{\partial \bar{D}}{\partial t}$$

Maxwell's Second Equation states that a magnetic field is generated by the flow of electric current:

(2) $$\bar{\nabla} \times \bar{H} = \bar{J} + \frac{\partial \bar{D}}{\partial t}$$

Maxwell's Third Equation states the existence of a closed-loop property of electric displacement in the presence of electric charge density:

(3) $$\bar{\nabla} \times \bar{D} = q$$

Maxwell's Fourth Equation states that the magnetic flux forms a closed loop in the absence of free magnetic currents:

(4) $$\bar{\nabla} \times \bar{B} = 0$$

Notation:

E = Electric field vector (V/m)

B = Magnetic field vector (Tesla)

J = Electric current density vector (A/m²)

D = Electric displacement vector (C/m²)

H = Magnetic field intensity vector (A/m)

q = Electric charge density (C/m³)

t = Time (seconds)

Ground Penetrating Radar (GPR) is a highly effective method for detecting subsurface conditions up to a depth of 10 meters with high-resolution results, making it frequently used in fields such as archaeology, civil engineering, and subsurface utility mapping.

Resolution refers to the ability to distinguish between two distinct objects located close to each other. It is crucial in determining spatial attributes such as position, size, shape, and thickness. High resolution can only be achieved using shorter wavelengths, which in turn require higher operating frequencies.

Fundamentally, GPR operates based on the reflection of signals. Electromagnetic waves are emitted from the transmitting antenna (Tx) into the target medium, traveling through the material at a velocity primarily determined by the material's permittivity.

A portion of the wave is reflected or scattered back to the surface when encountering a boundary with differing electrical properties, while the remaining energy continues downward until it encounters another subsurface object. The reflected signal is then captured by the receiving antenna (Rx), and the system produces an output in the form of a radargram.

## SYSTEM COMPONENTS

The component system used in the GPR data acquisition process consists of four main parts: the antenna, control unit, display unit, and power supply. The antenna functions as both the transmitter and receiver of the electromagnetic waves that propagate beneath the surface. Several types of antennas have been developed by Geoscanners, one of which is the GCB model antenna.

The control unit serves to convert the analog signals received from the antenna into digital signals, which are then transmitted to the display unit. Generally, there are two types of control units compatible with the GCB antenna model: the Akula 9000B and Akula 9000C.

Each GPR manufacturer provides specialized applications or software integrated with their GPR systems for both data acquisition and processing. Geoscanners has developed two main software tools for GPR users: GAS XPC and GPRSoft. In comparison, GSSI RADAN 7, developed by GSSI, is also used as a benchmark software for data processing.

## RESULTS

This section presents the results and analysis based on the processed data. The data analysis aims to identify the subsurface layer features beneath the road pavement, as interpreted from the radargram outputs. Additionally, a comparison is made between the results obtained from two different data processing software tools: GPRSoft and GSSI RADAN 7.

### Point A (Candi Raya Street) (Flexible Pavement)

(a) Point A1 (Good Surface Road) (GPRSoft)

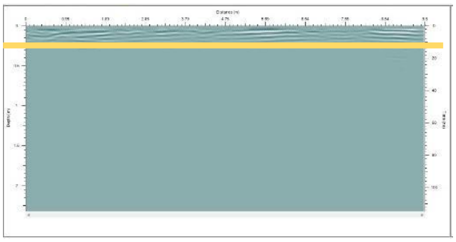

(b) (GSSI RADAN7)

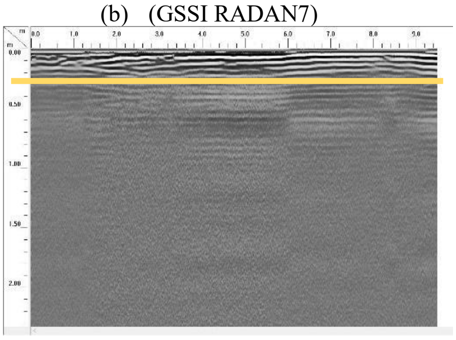

**FIGURE 1.** (a) & (b) Processed Result of Point A1

(a) Point A2 (Cracked Surface Road) (GPRSoft)

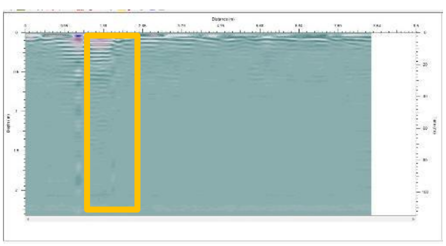

(b) (GSSI RADAN 7)

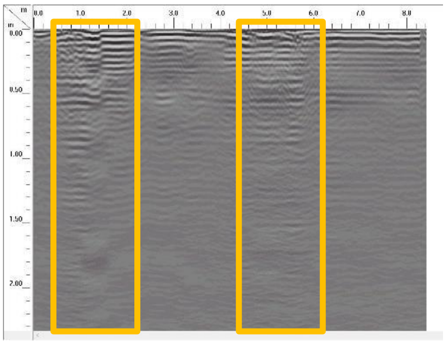

**FIGURE 2.** (a) & (b) Processed Result of Point A2

Based on the results of data processing using both GPRSoft and GSSI RADAN 7, a noticeable difference can be observed in the visibility of subsurface layers—GSSI RADAN 7 provides clearer stratigraphic details compared to GPRSoft. In sections with damaged road surfaces, the data can be interpreted as indicating weak zones or layer failures. Furthermore, GSSI RADAN 7 reveals additional anomalies not visible in GPRSoft.

For road segments with good surface conditions, the processed data also shows differences. GSSI RADAN 7 detects an anomaly that may indicate a weak subsurface layer, which is not as clearly represented in GPRSoft. However, in segments with damaged road surfaces, both software tools identify anomalies at approximately the same locations, showing no significant difference in the interpretation of the damaged layer positions.

## CONCLUSIONS

It can be observed from the GPR data results for two types of road pavements—flexible and rigid—and two surface conditions—good and damaged—that the following conclusions can be drawn: for both pavement types (flexible and rigid), weak zones were identified in the sub-grade layer at multiple points along roads with damaged surfaces. In contrast, on roads with good surface conditions, differences in interpretation emerged; anomalies were detected in the sub-grade layer of the rigid pavement section, while no such anomalies were observed in the flexible pavement section.

Based on the GPR data interpretation, several differences were identified between the two software tools, GPRSoft and GSSI RADAN 7. Anomalies that were visible in GSSI RADAN 7 were not detected in GPRSoft. These differences also extended to the interpretation accuracy of pavement layer boundaries. Therefore, the use of more than one software tool can serve as validation and comparison, highlighting the necessity of using multiple applications to improve the accuracy of GPR data interpretation.

## REFERENCES


[1] Elfarabi, Widodo, A., & Syaifudin, F. (2017). Pengolahan Data Ground Penetrating Radar (GPR) dengan menggunakan software MATGPR R-3.5. 6(1).

[2] Feranie, S., Tohari, A., Karmila, I., & Puspitasari, A. D. (2023). Penerapan Metode GPR dan Geoteknik pada Kajian Jalan, Jembatan, dan Lereng. *Jurnal Sains dan Edukasi Sains*, *6*(2), 51-64.

[3] Lai, W. W. L., Derobert, X., & Annan, P. (2018). A review of Ground Penetrating Radar application in civil engineering: A 30-year journey from Locating and Testing to Imaging and Diagnosis. *Ndt & E International*, *96*, 58-78.

[4] Nugroho, U., & Susanto, N. C. J. (2023, June). Comparison of GPR (Ground Penetrating Radar) Penetration Results Using the GCB-400 Antenna on Flexible and Rigid Pavement. In *IOP Conference Series: Earth and Environmental Science* (Vol. 1203, No. 1, p. 012022). IOP Publishing.

[5] Solla, M., Pérez-Gracia, V., & Fontul, S. (2021). A review of GPR application on transport infrastructures: Troubleshooting and best practices. *Remote Sensing*, *13*(4), 672.

Jurnal Teknik Sipil & Perencanaan 26 (1) (2024) p 15 - 21

JURNAL TEKNIK SIPIL & PERENCANAAN

http://journal.unnes.ac.id/nju/index.php/jtsp/index

# Analysis of the Finite Element Method in Reinforcing Soft Soil using Geotextiles

Pranadya Krida Palgunadi[1 a)], Togani C U[2]

*Civil Engineering, Faculty of Engineering, Semarang State University, Semarang City, Indonesia;*
pranadya27@students.unnes.ac.id

[a)]Correspondence: pranadya27@students.unnes.ac.id

**SUBMITTED** March 24, 2025 **REVISED** March 24, 2025 **ACCEPTED** March 24, 2025

**Abstract.** This study focuses on the analysis of the finite element method for soft soil reinforcement using geotextiles in the Tambak Lorok area, Tanjung Emas Village, Semarang Utara District, Central Java. The research location was selected because this area is experiencing rapid economic and infrastructure development, but faces significant soil subsidence issues due to the high swelling-shrinking potential of clay soil. This subsidence negatively impacts building stability as well as the social and economic lives of the community. This study aims to evaluate the stability of fill soil with and without geotextile reinforcement using Plaxis 2D software. The research method used is quantitative, with analysis using Plaxis 2D to evaluate the stability of the original fill soil with and without geotextile reinforcement. The data used includes secondary data from government agencies and primary data from standard penetration tests (SPT) as well as interviews with local residents. This study is limited to the location on Tambak Mulyo Road, with aspects reviewed including the extent of soil subsidence and the safety factor of the fill. The software used is PLAXIS 2D, and Google Maps historical data and interview results are used for data validation. The analysis results show that the stability level of the original fill soil without geotextile tends to be lower, with significant soil settlement at the measurement point. Before the application of geotextile, the safety factor value of the fill soil was 1.407. After the application of geotextile with a tensile strength of 200 kN/m², the safety factor increased to 1.507. These results indicate that the use of geotextile is effective in enhancing the stability of fill soil in the Tambak Lorok area, North Semarang.

Keywords: Soil settlement, geotextile, safety factor, Plaxis 2D, Tambak Lorok

## BACKGROUND

In every civil engineering project, soil is an important element that cannot be ignored. Many problems that often arise in civil engineering structures in the field are caused by poor soil properties, such as high water content, high compressibility, and low bearing capacity. Some types of soil with these poor characteristics tend to undergo significant volume changes due to swelling and shrinkage. As the capital of Central Java, Semarang has experienced rapid development in the fields of economy, industry, and infrastructure. However, this development poses challenges, particularly regarding environmental sustainability. Some soil types with high potential for swelling and shrinkage are those that undergo significant volume changes when their moisture content varies. Such soils are typically clay soils containing minerals with high swelling capacity. Soil with these characteristics is often referred to as clay soil. Soil subsidence in Semarang affects the stability of infrastructure buildings and has widespread impacts on the social and economic lives of the community. Residents in areas prone to soil subsidence face risks of house damage, cracked roads, and disruptions to drainage and sanitation systems. This leads to increased repair and maintenance costs and can hinder regional economic growth. One of the common causes of building construction failure is land subsidence resulting from consolidation processes. This subsidence is caused by loads acting on the soil. If the subsidence occurs uniformly and is not excessive, it typically does not cause damage to buildings. However, if the subsidence occurs unevenly and excessively, it can lead to structural damage, disrupt building stability, and impair the aesthetics and comfort of building users. Research on land subsidence in Semarang is crucial for understanding the causes and mechanisms of land subsidence, as well as formulating effective strategies to mitigate its impacts. It is hoped that this research will contribute to the formulation of policies and practical steps to ensure environmental sustainability and improve the quality of life for the people of Semarang.

## LITERATUR REVIEW

1) Land Subsidence
Land subsidence is the phenomenon of a decrease in ground elevation due to natural factors or human activities. Natural factors causing land subsidence include natural sediment compaction, soil consolidation, and tectonic and volcanic activity. Anthropogenic factors contributing to this phenomenon include excessive groundwater exploitation, infrastructure loads, and land use changes such as reclamation and agriculture. Land subsidence can be classified into two main types: immediate settlement and consolidation settlement. Immediate settlement occurs due to direct loads on elastic soil and is difficult to predict, while consolidation settlement is caused by changes in soil volume due to the release of pore water over a certain period of time.

2) Safety Factor
The safety factor in geotechnical engineering is an important parameter used to assess the stability of soil embankments against potential failure. This factor is calculated as the ratio between the available shear strength of the soil and the shear stress acting on the embankment. In this study, the safety factor was analyzed using the finite element method with PLAXIS 2D software. Calculations were performed by identifying weak planes in the soil layers, then gradually reducing the cohesion and friction angle values until reaching critical conditions.kritis.

**TABLE 1.** Recommended Safety Factor Values for Rock Slopes
(Source: SNI 8460:2017)

| Rock Slope Conditions | Recommended Safety Factor Values |
|---|---|
| Long-Term Conditions | 1,5 |
| Short-Term Conditions | 1,3 |

3) Geotextile
Geotextile is a geosynthetic material in the form of textile made from synthetic fibers, with high flexibility, and resistant to chemical reactions and weather conditions. In civil engineering, geotextile functions as a separation layer, filtration layer, drainage layer, soil reinforcement, and moisture barrier. The use of geotextiles in civil engineering projects offers several key benefits, such as improving soil stability in high embankments or slopes, reducing the risk of landslides, and enhancing infrastructure resistance to deformation caused by dynamic loads. Additionally, geotextiles aid in soil compaction and reduce erosion in soft soil layers.

**FIGURE 1.** Non-woven geotextile
(Source : Polyfabrics.com.au)

## RESEARCH LOCATION

This research was conducted in Tambak Lorok Village, Tanjung Emas Subdistrict, Semarang Utara District, Central Java, which is a coastal area with a high rate of land subsidence. Land subsidence in Tambak Lorok has serious impacts on the lives of the community, including increased frequency of tidal flooding, damage to buildings, and disruptions to drainage and sanitation systems. Therefore, this study focuses on analyzing the stability of fill soil reinforced with geotextiles using PLAXIS 2D software to mitigate the negative impacts of land subsidence and enhance the safety factor of the fill.


**FIGURE 2.** Research Location

## METHOD

This study uses quantitative methods, which focus on processing numerical data with statistical analysis to obtain objective and measurable results. The data used consists of primary and secondary data.

1. Data Collection Method
   a) Primary data was obtained through standard penetration tests (SPT) to analyze the geotechnical characteristics of the soil at the research site.
   b) Secondary data was obtained from government agencies, including geological maps, land subsidence data, and information related to geotechnical conditions in the research area.
2. Data Analysis Method
   This study uses PLAXIS 2D software, based on the finite element method, to simulate the stability of soil fill with and without geotextile reinforcement. The analysis includes:
   a) Determination of soil subsidence values at various measurement points.
   b) Evaluation of the safety factor of soil fill before and after geotextile reinforcement.

## RESARCH RESULTS

This section explains the results and analysis based on the data processing that has been carried out. Data analysis was performed to determine the settlement values and safety factors of the embankment before and after reinforcement with 200 kN/m tensile strength geotextile using PLAXIS 2D.

1. Settlement values before geotextile reinforcement

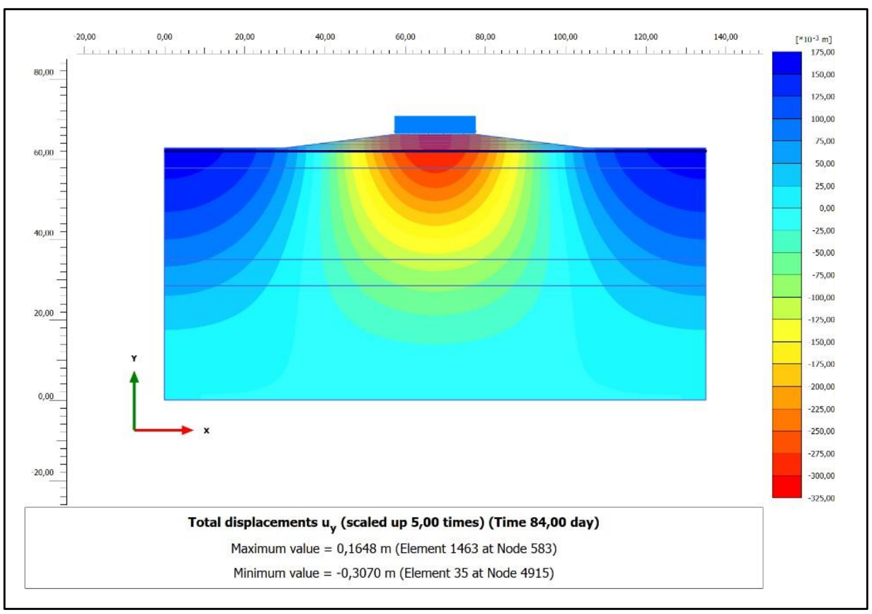


**FIGURE 3.** Value of the heap reduction before being given geotextile reinforcement

2. Safety factors before being given geotextile reinforcement

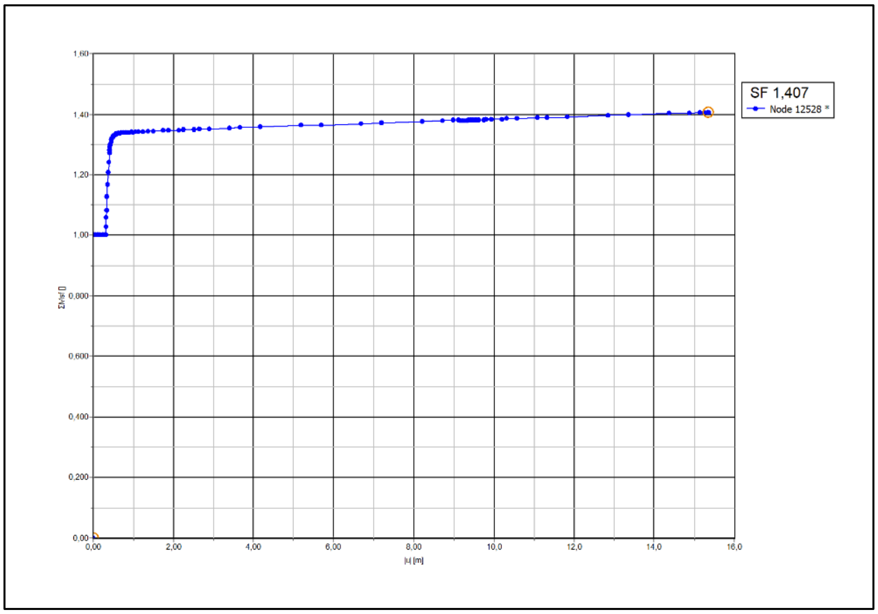


**FIGURE 4**. Graph of the safety of the stockpile factor before being reinforced with geotextiles

From the results of the analysis of the soil pile before being given the above geotextile reinforcement, a decrease value of 0.3070 m and a safety factor value of 1.407 were obtained. Then a stockpile analysis was carried out with geotextile reinforcement with a tensile strength specification of 200 kN/m.

3. Degradation value after being reinforced with 200 kN/m geotextile reinforcement

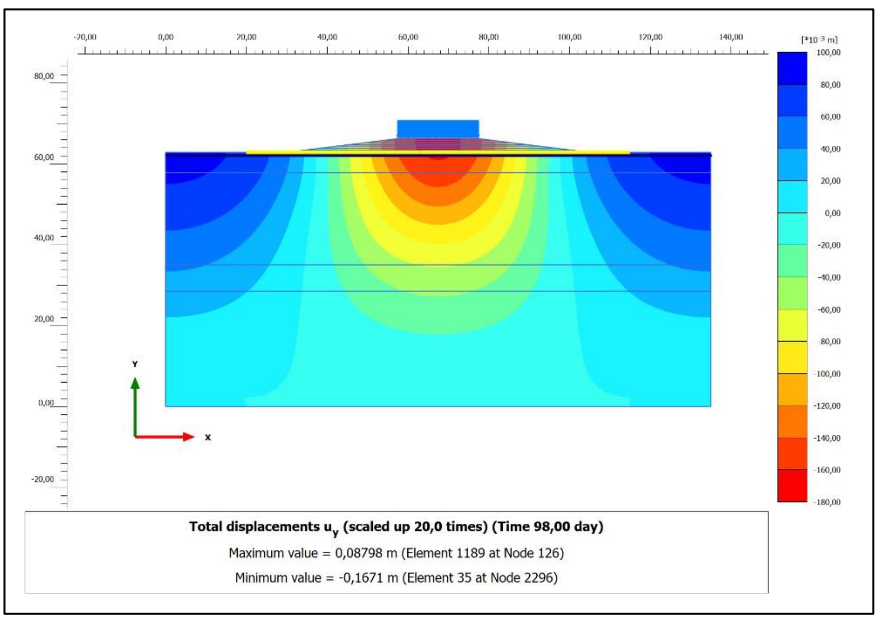


**FIGURE 5.** The value of the downfill after being reinforced with 200 kN/m geotextiles.

4. Safety factor after being reinforced with 200 kN/m geotextile

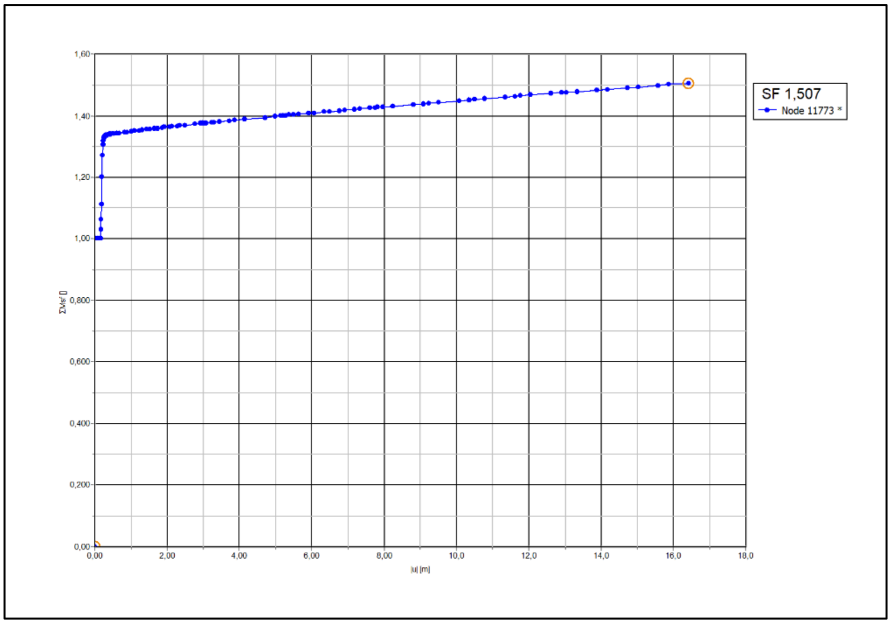


**FIGURE 6.** Graph of the safety of the stockpile factor after being reinforced with 200 kN/m geotextile

In the analysis of the heaps after being given geotextile reinforcement with a tensile strength specification of 200 kN/m, a decrease value of 0.1671 m and a safety factor value of 1.507 were obtained.

## CONCLUSION

Based on the analysis of the value of the decline and safety factors that have been carried out on the soft soil of Kampung Tambak Lorok, North Semarang, Semarang City, Central Java, it can be concluded that in the heap before being given geotectile reinforcement there was a decrease of 0.3070 meters in the vertical direction and a safety factor of 1.407 was obtained, referring to SNI 8460:2017 for long-term construction safety factors the value above is not qualified or it can be said that the heapland is unstable. Then for the stockpile after being strengthened with a geotextile with a tensile strength of 200 kN/m, a decrease value of 0.1671 m was obtained in the vertical direction and a safety factor value of 1.507, referring to SNI 8460:2017 for long-term construction in the analysis of the stockpile after being given the reinforcement of the geotextile of 200 kN/m can be said to be stable.

## PENAFIAN



## AVAILABILITY OF DATA AND MATERIALS

The data and materials used in this article are obtained from relevant and accountable sources. However, the author does not guarantee the accuracy, completeness, or novelty of the information presented. Fully use of the data and materials in this article be the responsibility of the reader If required, the reader may contact the author for further information regarding the availability of data and related materials.

## THANKS

With great respect, I would like to thank Prof. Dr. Rini Kusumawardani, S.T., M.T., M.Sc., for the guidance, knowledge, and direction that has been given during the process of compiling this article. The support and insight that you provide are very helpful in understanding and developing the topics discussed. Hopefully the knowledge that has been taught will be a valuable provision for me and other colleagues.

Thank you also to friends who have provided support, discussion, and enthusiasm in completing this article. The togetherness and cooperation that has been established is very meaningful in this academic journey.


## REFERENCES


[1] Abidin, HZ, Andreas, H, Gumilar, I, Sidiq, TP, & ... (2013). Land subsidence in coastal city of Semarang (Indonesia): characteristics, impacts and causes. *... , Natural Hazards and i...*, Taylor &Francis, https://doi.org/10.1080/19475705.2012.692336

[2] Abidin, HZ, Djaja, R, Darmawan, D, Hadi, S, Akbar, A, & ... (2001). Land subsidence of Jakarta (Indonesia) and its geodetic monitoring system. Natural Hazards, Springer, https://doi.org/10.1023/A:1011144602064

[3] Holzer, TL, & Galloway, DL (2005). Impacts of land subsidence caused by withdrawal of underground fluids in the United States., pubs.geoscienceworld.org, https://pubs.geoscienceworld.org/gsa/books/edited-volume/921/chapter/4847138

[4] Kasfari, R., Yuwono, B. D., & Awaluddin, M. (2018). Pengamatan Penurunan Muka Tanah Kota Semarang Tahun 2017. Jurnal Geodesi Undip, 7(1), 120-130.

[5] Melle, D. A., & Jatmiko, P. (1999). Pemakaian Geotekstil sebagai Perkuatan Tanah Lunak pada Badan Jalan.

[6] Siswanto, A. B., Wijaya, U., & Widawati, E. (2023). Perbaikan Tanah Lunak Untuk Konstruksi Jalan Pada Proyek Jalan Lingkar Utara Brebes Tegal. Journal Of Civil Engineering And Technology Sciences, 2(1), 31-43.

[7] Umum, K. P., & Rakyat, P. (2017). Manual Perkerasan Jalan. Direktorat Jenderal Bina Marga. Jakarta.

Jurnal Teknik Sipil & Perencanaan 26 (1) (2024) p 22 - 28

UNNES JOURNALS

JURNAL TEKNIK SIPIL & PERENCANAAN

http://journal.unnes.ac.id/nju/index.php/jtsp/index

# Correction of SPT (Standard Penetration Test) between Comparison of Energy Measurement in the Field and Seed Method (1985)

Muhammad Farhan Syahputra[1, a)] and Togani Cahyadi Upomo[1, b)]

[1]S1 Civil Engineering Study Program, Faculty of Engineering, Semarang State University, Semarang, Indonesia, Postal Code 50229;
muhfarhansyahputra@students.unnes.ac.id
[2]*Civil* Engineering S2 Study Program, Faculty of Engineering, Semarang State University, Semarang, Indonesia, Postal Code 50229;
togani.cahyadi@mail.unnes.ac.id

[*)]*Email: muhfarhansyahputra@students.unnes.ac.id*

**Abstract.** The use of *the Standard Penetration Test* (SPT) method has a very important role in the field of geotechnical engineering, especially in obtaining information related to soil characteristics under the surface. The data obtained from the SPT test is widely used in various applications, one of which is slope stability analysis, especially in areas with high potential for landslide disasters. This research was conducted as a form of the author's scientific contribution in highlighting the difference in energy produced by the SPT tool in the field compared to the results of the theoretical calculation approach. The research methodology includes the collection of data from the results of tax return testing in the field, which is then analyzed using the calculation method of the Seed method (1985). In the energy measurement in the field, *the energy ratio* (ER) was obtained of 56.3-77.7%. The average energy measurement at the BH-1, BH-2, and BH-3 test points was obtained at 70.9% each; 70.4%; and 64.8%. The results of the correction comparison showed the difference between the energy return from the energy measurement test in the field and the theoretical calculation. At depths of 0-10m it is 7-32% and at depths of 10-20m it is 7-15%. Corrections using the Seed method (1985) showed a relatively higher error rate compared to the results of direct energy measurements in the field. Taking this into account, the use of energy data obtained directly is considered more representative of actual conditions in the field and more reliable in the correction value of tax returns.

Keywords : *Standard Penetration Test*; Energy Measurement SPT; Seed Method

## INTRODUCTION

Testing with *standard penetration test* (SPT) is quite popular and widely applied in the geotechnical field. The SPT test was carried out by freely dropping a hammer weighing 63.5 kg from a height of 76 cm, thus pushing the standard penetration tool into the ground (Ji et al., 2023). The energy that falls depends on several factors such as the type of hammer, operator, SPT testing method, drill pipe length and test depth, so some researchers recommend standardizing the SPT energy efficiency ratio of 60% as a benchmark (Schmertmann & Palacios, 1979; Seed et al., 1985). Seed et al. (1985) recommend the correction of energy from the SPT test which is hereinafter referred to in this article as the Seed (1985) method.

According to Adam (1971), it shows that *stress wave* consistency can be used in predicting the force and speed of the SPT drill rod. Schmertmann & Palacios (1979) used *wave theory* to analyze the SPT *stress wave measurement*. Morgano & Liang (1992) adopted *accelerometers* and *strain gauges* used for SPT testing systems. Because they measured the impact velocity and *stress wave (FV) energy*, the reduced fall height did not affect their conclusions. There is a significant difference between *hammer impact energy* and *stress wave energy* associated with drill rod length, thus increasing the benefits of *stress wave measurement* and reducing the importance of *impact velocity*.

This article discusses the difference between the results of correction of SPT-N using direct energy measurement in the field and the Seed method (1985). Measurements were taken in the Petobo landslide area, Palu with the measurement location shown in Figure 1. In this study, the energy measurement of SPT using *SPT Analyzer* products from *Pile Dynamics, Inc.* The measured energy will be automatically recorded in the logger.

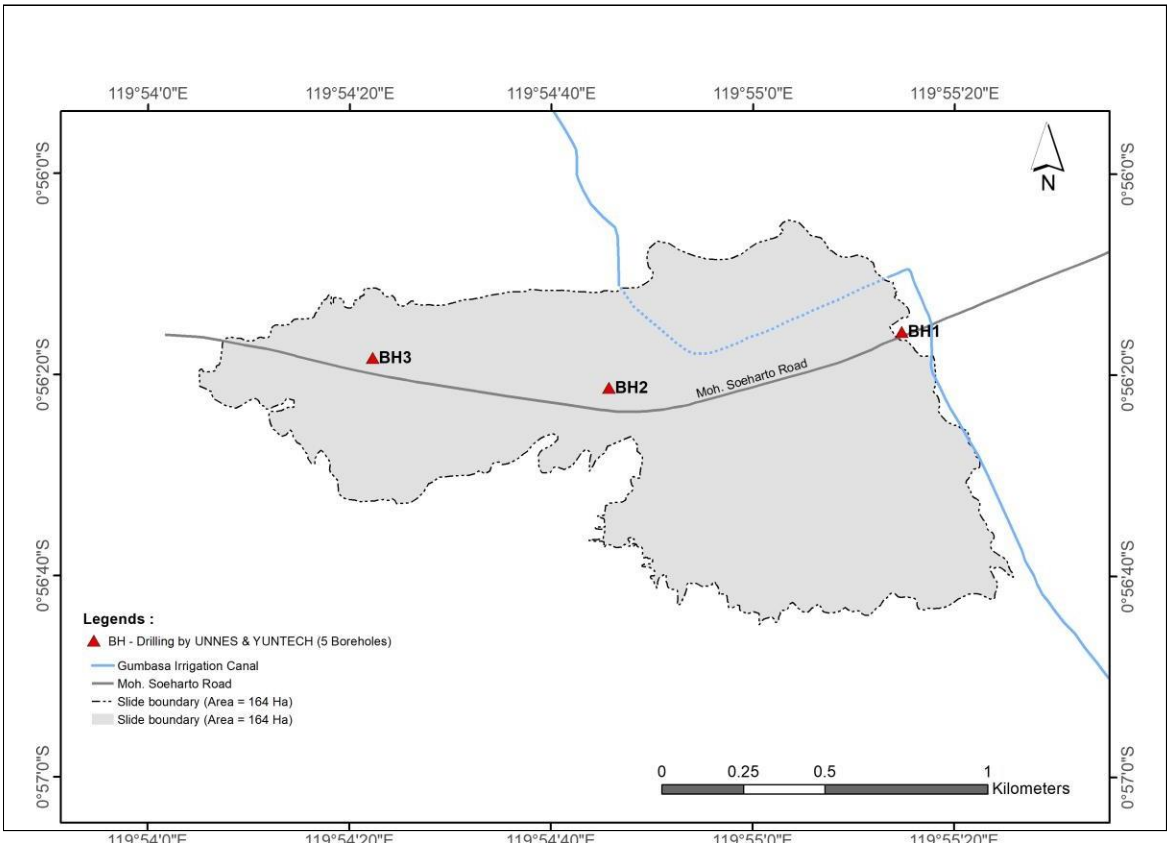


**FIGURE 1.** Location of drilling points and SPT testing

# METHOD

In general, the equation of the energy efficiency ratio can be seen in the following equation:

$$N60 = \frac{ER}{60} \times N \quad (1)$$

with N60 = the standard penetration test that has been corrected against energy (blows/feet) and N = the number of strokes resulting from the SPT test (blows/feet).

Correction to the energy value can be made by measuring energy directly in the field using *accelerometers* and *strain gauges* or referring to the Seed method (1985).

In addition to corrections to energy, tax returns also need to be corrected to *overburden pressure*. The concept of N1 is the value of the tax return that is corrected to *the overburden pressure* (Seed, 1987). The equation of the tax return value after being corrected for *overburden pressure* and energy is shown in equation 2.

$$(N1)_{60} = N.\ CN.\ 60\% \quad (2)$$

with $(N1)_{60}$ = standard penetration test of corrected N values for energy and overburden stress (blows/feet), CN = correction of overburden pressure *voltage factor.*

The CN value commonly used for correction of *overburden pressure* refers to the equation proposed by Liao and Whitman (1986) as seen in equation 3.

$$C_N = \left(\frac{Pa}{\sigma' VC}\right)^{0.5} \leq 1.7 \quad (3)$$

According to Seed et al. (1985) in determining $(N_1)_{60}$, the calculation was carried out using the N-SPT correction factor. To get the value, the following formula is used:

$$(N1)_{60} = CN \times CE \times CB \times CR \times CS \times N \quad (4)$$

with CN = Normalization factor N to *overburden pressure,* CE= correction factor of *hanmmer energy ratio,* CB= correction factor of drill hole diameter, CR=correction of drill rod length, CS= correction factor of sample, N= SPT-N (blows/feet)

**TABLE 1.** N-SPT Correction Factor
(Youd et al., 2001)

| Factor | Equipment variables | Symbol | Correction |
|---|---|---|---|
| *Overburden pressure* | - | CN | |
| *Overburden pressure* | - | CN | |
| *Energy Ratio* | Doughnut Hammer | CE | 0.5-1.0 |
| *Energy Ratio* | Safety Hammer | CE | 0.7-1.2 |
| *Energy Ratio* | Automatic-trip-Doughnut type Hammer | CE | 0.8-1.3 |
| *Borehole diameter* | 65-115 mm | CB | 1 |
| *Borehole diameter* | 150 mm | CB | 1.05 |
| *Borehole diameter* | 200 mm | CB | 1.15 |
| *Rod Length* | <3 mm | CR | 0.75 |
| *Rod Length* | 3-4 mm | CR | 0.8 |
| *Rod Length* | 4-6 mm | CR | 0.85 |
| *Rod Length* | 6-10 mm | CR | 0.95 |
| *Rod Length* | 10-30 mm | CR | 1 |
| *Sampling method* | *Standard sampler* | CS | 1 |
| *Sampling method* | *Sampler without Liners* | CS | 1.1-1.3 |

Figure 2 shows the drilling process of SPT testing with energy measurement. Drilling uses a core barrel with a size of 76mm. The SPT test is carried out using a rope with *a doughnut hammer* and manually dropped, resulting in a non-constant fall height. Under the anvil, a pipe is installed with *accelerometer* sensors and *strain gauges* and connected to a *logger* so that the data obtained will be recorded automatically. When *the hammer* is dropped from a height of 76 cm, then the energy can be estimated from the *accelerometer sensor* and *strain gauges.*

**FIGURE 2.** Field Tax Return Testing: (A) Doughnut Hammer; (B) Ram Energy (Upomo & Chang, 2023)

In this study, researchers took SPT-N data in the Petobo Village area, Palu City, Central Sulawesi. As a limitation of the problem, it is specified that the diameter of the analyzed pile is 65-115mm. In this study, the research process is divided into several stages, including the following:

- The data collection stage, this stage is the stage of collecting SPT-N field test data in the field by measuring energy. SPT-N was carried out at 3 points in the Petobo avalanche area, Palu City, Central Sulawesi.
- The analytical and data processing stage, this stage processes the data from energy measurements in the field and compares it with the theoretical calculations proposed by Seed (1985).
- The calculation of the error value is carried out by referring to the following equation:

$$\chi = \frac{(N1)_{60\text{ S. S.}}(N1)_{60\text{ Seed(1985)}})}{(N1)_{60\text{measurement}}} \times 100\% \quad (5)$$

with $\chi$= total error, $(N1)_{60\text{measurement}}$= SPT-N result of overburden voltage correction and energy measurement in the field, $N(N1)_{60\text{ Seed(1985)}}$ = SPT Seed method (1985)

## RESULT

At the BH-1 point, energy data collection was carried out at a depth between 4.55 to 22.55 meters, with an average energy recorded of 70.9%. Meanwhile, in BH-2, measurements were carried out at a depth of 9.05 to 22.55 meters and produced an average energy value of 70.4%. For the BH-3 point, the test was carried out in a depth range of 6.05 to 22.55 meters, with an average energy obtained of 64.8%. In general, the measured energy value is more than 60%, there are only 3 data with a value of less than 60% as seen in Figure 3.

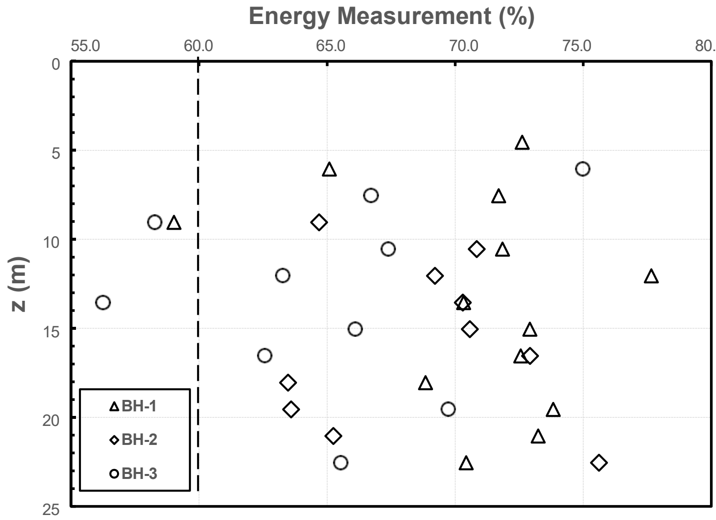


**FIGURE 3.** Energy measurements are made at the specified depth at the test point.

Energy measurement is directly considered as a reference in the comparison of the corrected SPT-N values against overburden and energy pressure. Energy correction refers to field testing, the Seed method (1985) and the average of energy measurements at drill points in BH-1, BH-2 and BH-3. Figure 4~6 is the result of a comparison between energy measurement in the field, the seed method (1985) and the average energy measurement.

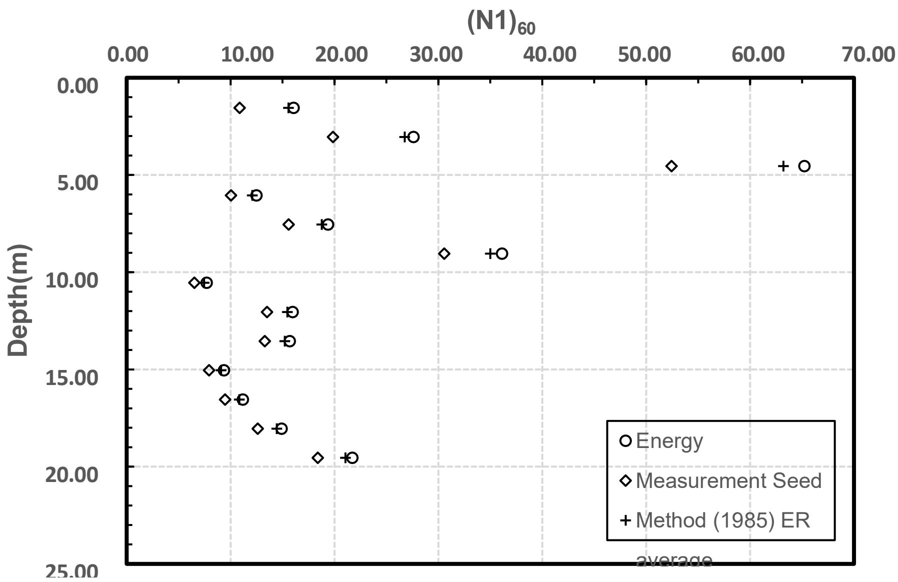


**FIGURE 4.** Value (N1)60 with energy measurement correction, Seed method (1985), and BH-1 mean energy correction

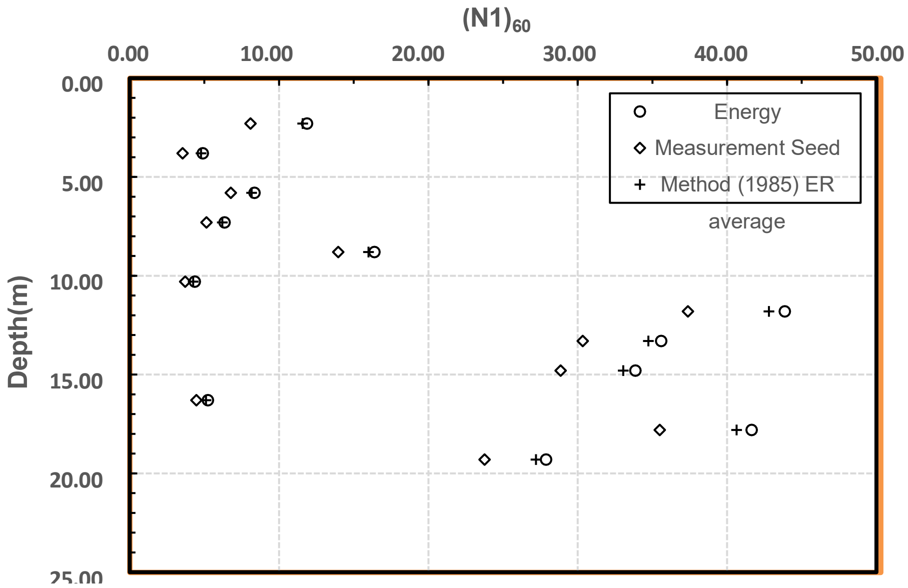


**FIGURE 5.** Value (N1)60 with energy measurement correction, Seed method (1985), and BH-2 mean energy correction

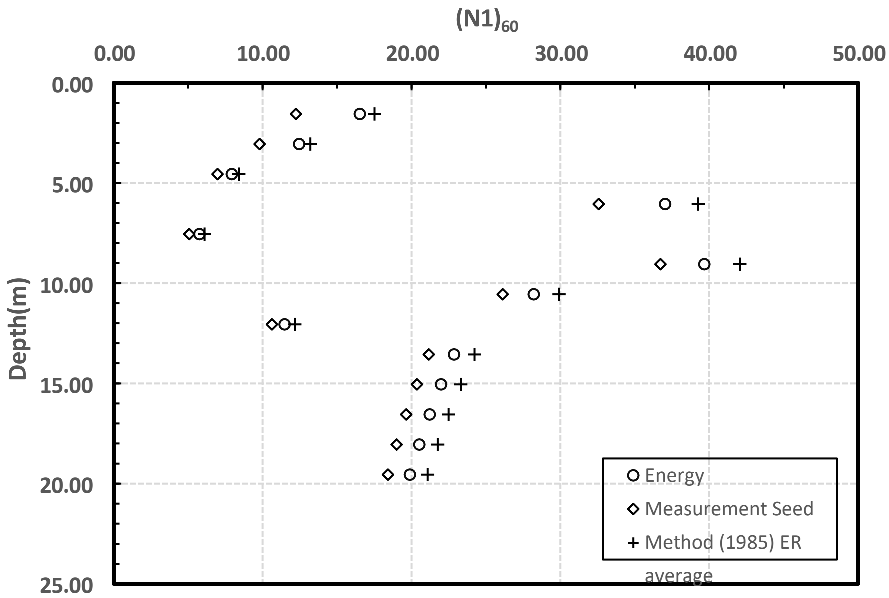


**FIGURE 6.** Value (N1)60 with energy measurement correction, Seed method (1985), and BH-3 mean energy correction

Figure 4~6 shows the same trend in BH-1, BH-2 and BH-3. The correction using energy measurement gave a higher value of $(N_1)_{60}$ when compared to the Seed method (1985) and was quite close to the average energy correction. If the assumption that direct energy measurements are correct, then the error rate of the Seed (1985) method and the average approach on BH-1 with depths between 0–10 m ranges from 15% to 32%. Meanwhile, at a depth of 10–20 m, the *error* value reaches about 15%. In contrast, when comparing direct energy measurements with average energy, the *error* was relatively smaller, at about 3% for an overall depth of 0–20 m.

The value $(N1)_{60}$ at the BH-2 point that the value at a depth of 0–10 m indicates the error rate of the Seed method (1985) and the average approach at a depth of 10–20 m is in the range of 14% to 31%, while at a depth of 10–20 meters, the error value recorded reaches 14%.

When compared to the average value of energy, the direct energy measurements show a much smaller error rate, which is about 2% for the entire depth of 0-20 m

The value of $(N1)_{60}$ at the BH-3 point at a depth of 0–10 m in a comparison between the values from direct energy measurements and the Seed (1985) method showed an error rate of between 25% to 7%. Meanwhile, for a depth of 10–20 m, the *error* difference was recorded at 7%. However, when compared to the average value of energy, direct energy measurements show a much smaller error rate, which is about -6% at depths of 0–20 m.

## CONCLUSION

Field energy measurements on the Standard Penetration Test (SPT) test show that the actual energy value that occurs during the test can differ significantly from the theoretical assumed standard energy value by 60%. From the data obtained at three test points, namely BH-1, BH-2, and BH-3, it can be seen that the energy recorded in the field ranges from 56.3% to 77.7%. This shows that there is considerable variation in the energy measured.

The increase in energy value has a direct impact on the results of the tax return value obtained. The higher the percentage of energy given into the ground, the smaller the value of the hit recorded. The results of the analysis of the correction of SPT values with two approaches—direct energy measurement in the field and the theoretical correction method based on Seed (1985) showed a significant difference, especially at a depth of 0–10 meters. Corrections using the Seed method (1985) tend to produce greater errors when compared to energy measurements in the field. The error value recorded in the Seed (1985) approach ranged from 7% to 32%. Therefore, the assumption of energy in the Seed method (1985) is larger, which gives more conservative results, so in the tax return test it is better to measure the amount of energy for correction.

## REFERENCE


[1] Adam, J. (1971). Discussion of "The standard penetration test" by V.F.B. de Mello. Proceedings of the 4th Panamerican Conference on Soil Mechanics and Foundation Engineering, 3, 82–84.

[2] JI, P., YANG, J., ZHANG, N., ZHAI, Q., LI, M., WANG, Y., SHEN, T., & SATYANAGA, A. (2023). ENERGY MEASUREMENT IN STANDARD PENETRATION TESTS. SUSTAINABILITY, 15(6), 4763. HTTPS://DOI.ORG/10.3390/SU15064763

[3] Morgano, C. M., & Liang, R. Y. (1992). Energy transfer in SPT–rod length effect. Proceedings of the 4th International Conference on the Application of Stress- Wave Theory your Piles, 121–127. https://www.pile.com/wp content/uploads/2017/03/EnergyTransferInSPTRodLengthEffect.pdf

[4] Schmertmann, J. H., & Palacios, A. (1979). Energy Dynamics of SPT. Journal of Geotechnical Engineering Division, Proceedings of the American Society of Civil Engineers 105(GT8), 909–926.

[5] Seed, H. B. (1987). Design problems in soil liquefaction. Journal of Geotechnical Engineering, 113(8), 827–845

[6] Seed, H. B., Tokimatsu, K., Harder, L. F., & Chung, R. M. (1985a). Influence of SPT Procedures in Soil Liquefaction Resistance Evaluations. Journal of Geotechnical Engineering, 111(12), 1425–1445. https://doi.org/10.1061/(ASCE)0733-9410(1985)111:12(1425)

[7] Seed, H. B., Tokimatsu, K., Harder, L. F. Jr., & Chung, R. (1985b). Influence of SPT procedures in soil liquefaction resistance evaluations. J.Geotechnical Eng., ASCE 111(12), 1425–445.

[8] Head, T. C., & Chang, M. (2023). A Study on the Causes and Mechanism of Soil Liquefaction Flowslide in Petobo during 2018 PaluDonggala Indonesia Earthquake. Graduate School of Engineering, Science and Technology, National Yunlin University of Science & Technology Doctoral Dissertation.

[9] YOUD, T. L., IDRISS, I. M., ANDRUS, R. D., ARANGO, I., CASTRO, G., CHRISTIAN, J. T., DOBRY, R., FINN,W. D. L., JR, L. F. H., HYNES, M. E., ISHIHARA, K., KOESTER, J. P., LIAO, S. S. C., III, W. F. M.,MARTIN, G. R., MITCHELL, J. K., MORIWAKI, Y., POWER, M. S.,ROBERTSON, P. K., ... II, K. H.S. (2001). Liquefaction Resistance Of Soils: Summary Report From The 1996 Nceer And 1998 NCEER/NSF Workshops On Evaluation Of Liquefaction Resistance Of Soils. Journal Of Geotechnical And Geoenvironmental Engineering, 817–833.

Jurnal Teknik Sipil & Perencanaan 26 (1) (2024) p 29 - 33

UNNES JOURNALS

**JURNAL TEKNIK SIPIL & PERENCANAAN**

http://journal.unnes.ac.id/nju/index.php/jtsp/index

# Interpretation of Ground Penetrating Radar (Gpr) to Determine the Depth of Pipe Objects in the Sandbox

Dwi Sri Wahyudi [a)] and Rini Kusumawardani[1, b)]

[1]*Civil Engineering, Faculty of Engineering, Semarang State University, Semarang City, Indonesia;*
dwisriwahyudi@students.unnes.ac.id
[1]*Civil Engineering, Faculty of Engineering, Semarang State University, Semarang City, Indonesia;*
rini.kusumawardani@mail.unnes.ac.id

[a)]Correspondence: dwisriwahyudi@students.unnes.ac.id

**Abstract.** Ground Penetrating Radar (GPR) is a non-destructive inspection technology that utilizes electromagnetic (EM) waves to map subsurface structures. This study focuses on estimating the diameter and depth of buried cylindrical objects, especially pipes, using GPR. This research was carried out through laboratory experiments using a box filled with dry sand. GPR data is processed using matGPR software to analyze hyperbolic reflections generated by buried objects. matGPR is software used for mathematical calculations of all three software. The speed of the EM wave is calculated based on the dielectric properties of the sand, and the depth and diameter of the pipe are estimated using a mathematical model derived from hyperbolic reflection. The results showed that the pipe depth estimate had a low error percentage, generally below 5%, which indicated high accuracy in GPR measurements, pipe A showed an estimated depth of 16.2 cm with the result obtained an error percentage of 1.8%, pipe B showed an estimated depth of 15.3 cm with the result obtained an error percentage of 1% and pipe C showed an estimated depth of 13.7 cm with the result obtained The error percentage is 2.2 %.The study concludes that GPR is an effective tool for estimating the depth of buried objects, especially in a controlled environment such as a sandbox. However, factors such as burial depth, pipe material, and dielectric properties of the medium can affect the accuracy of the measurement. Future research should consider using varied pipe materials and deeper burial depths to further validate the reliability of this method under field conditions.

Keywords : Ground Penetrating Radar (GPR), hyperbolic reflection, buried pipe, depth estimation, sandbox experiment.

## BACKGROUND

*Ground Penetrating Radar* (GPR) can be used to detect the location of underground structures (Daniels, 2004). This method utilizes the principle that electromagnetic waves emitted from the surface to below the surface will be reflected at the surface boundary which has different electrical properties from the ground below the surface. Thus, this method can determine the location of surface boundaries and subsurface soil characteristics (Kanemitsu et al., 2024). The selection of the right antenna frequency depends on the project objectives (Burger, 1992). High frequencies produce higher resolution profiles at shallow depths, while low frequencies produce lower resolution profiles but can penetrate deeper (Ni et al., 2010). The use of GPR in civil engineering varies depending on the purpose of data collection, with each placing certain limitations on the design of effective GPR. For example, most buried pipes are within 1.5-2 m of ground level, but may have wide variations in size, materials (metallic or non-metallic), and environmental conditions, affecting the absorption and propagation speed of electromagnetic waves, as well as GPR

# LITERATURE REVIEW

*Ground Penetrating Radar* (GPR) utilizes electromagnetic waves, which are the propagation of electric field vibrations and magnetic fields that are perpendicular to each other in the direction of their propagation. The basic principle of this electromagnetic wave utilization is to measure the response of the soil to the propagation of electromagnetic waves, which involve alternating currents and magnetic fields (Kearey et al., 2002).

The speed of wave propagation can be calculated or measured through several techniques. However, if there is a significant horizontal variation in the electromagnetic properties of the soil or the moisture content below the surface, then the calculated velocity may only be valid at one calibration point (ASTM D6432-11, 2011). Accurate measurement of target depth relies heavily on an understanding of the propagation velocity of electromagnetic waves in the soil, which vary greatly and can lead to errors in depth estimates (Benedetto & Pajewski, 2015).

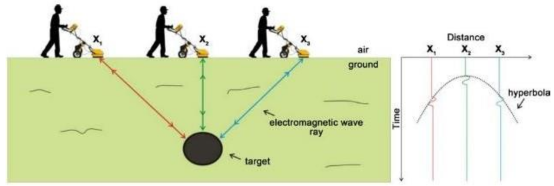


**FIGURE 1.** shows the position of the GPR profile and the resulting hyperbolic (Poluha et al., 2017)

The propagation speed of electromagnetic waves is influenced by soil type and moisture content, which often varies with depth from the surface depending on the nature of the rock mass (Jol, 2009). The waves reflected by buried objects have different electrical properties than ground. The time from signal transmission to reception (reflection time) is measured. When the instrument is scanned vertically into a buried pipe, the detected image appears as an upward convex satellite dish. Depth is estimated as the distance from the ground level to the highest intensity point at the parabolic peak. The depth of the pipe is calculated as follows (Kanemitsu et al., 2024):

$$\mathrm{D} = \frac{1}{2} \times (\mathrm{Vm.T}) = \frac{\mathrm{c}}{2\sqrt{\mathrm{\varepsilon r}}}\,.\mathrm{T} \qquad (1)$$

Information:

D = Depth of object (pipe) (m),
T = Reflection time of the target(s),
c = speed of Light in free space (3.00 x 108 m/s),
εr = relative dielectric constant,
Vm = velocity of electromagnetic waves (*velocity*) (m/s).

# COMPONENT SYSTEM

The component system used in the GPR acquisition process consists of four main parts, namely *antenna*, *control unit, display unit,* and *power supply*. *Antennas* function as *transmitters* and receivers of waves that propagate below the surface. There are several types of *antennas* developed by Geoscanner, in the study using the 1500 GCB model. The control unit serves to convert the analog signal received from the antenna into a digital signal, which is then sent to the display unit. The control unit is compatible with the antenna model 1500 GCB, i.e. the Akula 9000C. There are two main applications for GPR users developed by Geoscanner, namely GAS XPC, GPRSoft. For matGPR, which is *open-source software* that can be used through MATLAB, this is a comparative result. Wooden boxes containing dry sand and 3 pipes that were embedded are a medium for data collection in the laboratory.

# METHOD

*Radar Reflection Profiling* is a method in which antennas are moved simultaneously above ground level to collect data. In this method, the *two-way travel time* measured until it reaches the reflector is displayed on the vertical axis, while the distance traveled by the antenna during the scanning process is shown on the horizontal axis. In this way, information about the depth and position of the subsurface reflector can be obtained more clearly.

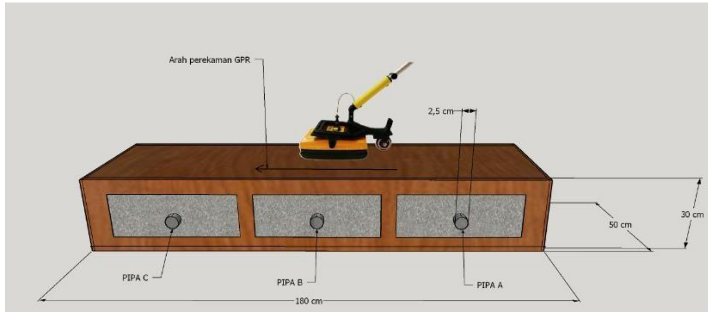


**FIGURE 2.** Illustration of GPR tool and sandbox and GPR data retrieval direction on sandbox

# RESEARCH RESULTS

In this section, it explains the results and analysis based on the data processing that has been carried out. Data analysis was carried out in order to find out the estimated depth and pipeline in the sandbox. Data processing uses *matGPR* software.

## Data processing results

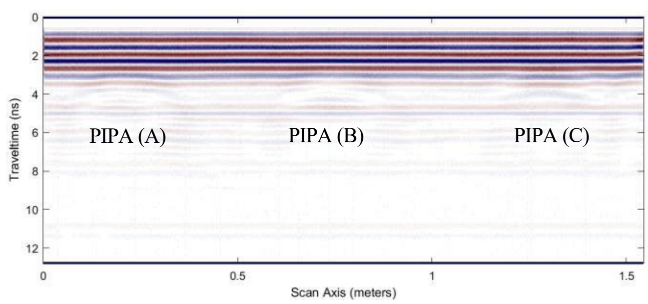


**FIGURE 3.** The results of the radar before the data are processed on matGPR (raw data) software

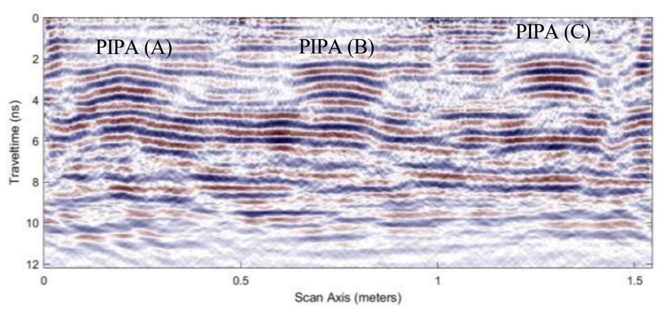


**FIGURE 4.** Radargram results after processing using matGPR software

**Calculation of the estimated depth and diameter of the wooden box**

**TABLE 1.** Results of depth estimation data for pipes A, B and C

| *Pipes* | *Actual Depth (cm)* | *Actual Deeph (m)* | *Velocity (drysands) (m/ns)* | *Time* | *Estimated depth (m)* | *Estimated depth (cm)* | *Error %* |
|---|---|---|---|---|---|---|---|
| A | 16,5 | 0,165 | 0,1278 | 2,54 | 0,162 | 16,2 | 1,8% |
| B | 15,5 | 0,155 | 0,1278 | 2,40 | 0,153 | 15,3 | 1,0% |
| C | 14 | 0,14 | 0,1278 | 2,14 | 0,127 | 13,7 | 2,2% |

**TABLE 2.** Time number data results on pipes A, B and C

| | Hyperbolic *time* value (ns) | | |
|---|---|---|---|
| Pipe | Above | Bawah | Δt |
| A | 2,54 | 2,70 | 0,165 |
| B | 2,40 | 2,57 | 0,168 |
| C | 2,14 | 2,31 | 0,169 |

# CONCLUSION

It can be seen that the results of GPR data for depth estimation using existing equations can produce an error percentage below 5%. i.e. pipe A has an *actual* depth of 16.5 cm and processing with software shows an estimated depth of 16.2 cm with the result obtained an error percentage of 1.8%. Pipe B has an *actual depth of 15.5 cm and processing with software shows an estimated depth of 15.3 cm with* the result of an error percentage of 1 %. Pipe C has an actual depth *of 14 cm and processing with software shows an estimated depth of 13.7 cm with the result obtained an error percentage of 2.2 %. This indicates that both data collection and processing have good accuracy results. GPR is an effective tool for estimating the depth of buried objects, especially in a controlled environment such as a sandbox.*

# PENAFIAN

This article aims to provide general information about civil engineering and is not professional advice. The author and publisher are not responsible for any errors, omissions, or repercussions of the use of this information. Always consult with the relevant engineer or expert before implementing the concepts discussed.

# AVAILABILITY OF DATA AND MATERIALS

The data and materials used in this article are obtained from relevant and accountable sources. However, the author does not guarantee the accuracy, completeness, or novelty of the information presented. The use of the data and materials in this article is entirely the responsibility of the reader If required, the reader may contact the author for further information regarding the availability of data and related materials.

# THANKS

Respectfully, I would like to express my deepest gratitude to the Soil Mechanics Laboratory of Semarang State University for the guidance, knowledge, and direction provided during the preparation of this article. The support and insights provided are invaluable in understanding and developing the topics discussed, so that they become valuable provisions for me and other colleagues in my academic and professional journey ahead. Again, thank you for all the help and dedication given.

I would also like to thank my friends for the support, discussion, and enthusiasm given in completing this article. The togetherness and cooperation that exists is very meaningful in this academic journey.

## REFERENCE


[1] ASTM D6432-11.: *Standard Guide for Using the Surface Ground Penetrating Radar Method for Subsurface Investigation* (2011)

[2] Benedetto, A. and Pajewski, L. (2015) *Civil engineering applications of ground penetrating radar*, *Springer transactions in civil and environmental engineering*. https://doi.org/10.1007/978-3-319-04813-0.

[3] Burger, H.R. (1992) *Exploration geophysics of the shallow subsurface*, *Prentice Hall eBooks*.http://library.uny.ac.id/sirkulasi/index.php?p=show_detail&id=5542& keywords=.

[4] Daniels, D.J. (2004) Ground penetrating radar. IET.

[5] Jol, H.M. (2009) Ground Penetrating Radar Theory and Applications, Elsevier eBooks. https://doi.org/10.1016/b978-0-444-53348-7.x0001-4.

[6] Kanemitsu, T., Morifuji, Y. and Kubota, K. (2024) 'Estimation of buried pipe depth in an artificial soil tank using ground-penetrating radar and moisture sensor,' Journal of Applied Geophysics, 220, p. 105283. https://doi.org/10.1016/j.jappgeo.2023.105283.

[7] Kearey, P., Brooks, M. and Hill, I. (2002) An introduction to geophysical exploration. John Wiley & Sons.

[8] Shihab, S., & Al-Nuaimy, W. (2005). Radius estimation for cylindrical objects detected by ground penetrating radar. Subsurface Sensing Technologies and Applications, 6(2), 151–166. https://doi.org/10.1007/s11220-005-0004-1

[9] Ni, S.-H. et al. (2010) 'Buried pipe detection by ground penetrating radar using the discrete wavelet transform,' Computers and Geotechnics, 37(4), pp. 440–448. https://doi.org/10.1016/j.compgeo.2010.01.003.

Jurnal Teknik Sipil & Perencanaan 26 (1) (2024) p 34 - 43

UNNES JOURNALS

JURNAL TEKNIK SIPIL & PERENCANAAN

http://journal.unnes.ac.id/nju/index.php/jtsp/index

# COMPARISON ANALYSIS OF LINEAR SCHEDULING METHOD (LSM) WITH PRECEDENCE DIAGRAMMING METHOD (PDM) ON DP MALL EXPANSION CONSTRUCTION PROJECT

M.Faizal Ardhiansyah, Anthonius Bara[a)], Galang Satrio and Agung Budiwirawan[1]

[1]*Civil Engineering, Faculty of Engineering, Semarang State University, Semarang City, Indonesia;*

[a)]Correspondence: anthoniusbara@students.unnes.ac.id

**Abstract.** The objective of this study is to analyze the comparison between the Linear Scheduling Method (LSM) and the Precedence Diagramming Method (PDM) in the DP Mall Expansion Project. The main focus of the research is to compare time efficiency, labor cost, and productivity in supporting construction with repetitive tasks. Project scheduling plays a crucial role in construction project development. In the construction industry, more focused scheduling is required for specific types of projects. This study uses a quantitative approach, specifically descriptive-comparative, to compare and analyze project scheduling using the Linear Scheduling Method (LSM) and the Precedence Diagramming Method (PDM). Scheduling analysis and preparation were carried out using Microsoft Excel and Microsoft Project. The scheduling was conducted under two scenarios: normal and accelerated. The analysis focused on architectural works, particularly regarding differences in project duration, labor wage costs, and the effectiveness of scheduling methods for repetitive work. The results show a significant difference between the two scenarios (normal and accelerated) in the Linear Scheduling Method (LSM). However, the accelerated scenario using both LSM and PDM produced the same total duration, number of workers, and labor wages due to the logical dependency relationships in PDM being applicable to LSM. LSM scheduling is more effective for repetitive work, while PDM is less effective for such projects. This research provides practical contributions for project managers in selecting the appropriate scheduling method according to the specific characteristics of a project. The results indicate that the Linear Scheduling Method (LSM) can be integrated into projects with repetitive tasks to achieve operational sustainability. This study presents a comprehensive analysis of the efficiency of scheduling methods in repetitive construction projects, contributing to project success in terms of time and cost.

Keywords : Project Scheduling, Repetitive Activity, Linear Scheduling Method (LSM), Precedence Diagramming Method (PDM)

## BACKGROUND

Project management plays a crucial role in the development of construction projects. Construction projects come in various types such as tunnels, high-rise buildings, housing developments, drainage systems, highways, and others (Rzepecki & Biruk, 2018). The type of project being undertaken influences the choice of project scheduling method. Scheduling refers to the detailed allocation of time for each activity or type of work in a construction project, from the beginning of the work to the completion (Utami & Nugraheni, 2023). In the construction industry, more focused scheduling is needed, which has proven to be more suitable for specific types of projects (Yamín & Harmelink, 2001). Improper scheduling can lead to problems in construction projects, such as delays, cost overruns, and failure to meet quality standards. Cost and time control are among the most critical issues in scheduling (Michin Jr. et al., 2013 in Muhammad et al., 2017).

Proper scheduling is the key to the success of a construction project, as project success is of utmost importance (Alafeef, 2025a). A successful construction project must be completed on time, within budget, and meet the required quality standards (Alafeef, 2025b). According to Yamín & Harmelink (2001), the most commonly known and used scheduling methods in construction projects include Network Planning Diagrams, Bar Charts/Gantt Charts, and Line of Balance (LOB). The most well-known LOB methods are the Linear Scheduling Method (LSM), Productivity Scheduling Method (PSM), Vertical Production Method (VPM), and Repetitive Scheduling Method (RSM) (Rzepecki & Biruk, 2018). In practice, bar charts and S-curves are the most frequently used scheduling tools in construction projects in Indonesia (F. J. Putra, 2019). Network Planning scheduling can provide resource management results, including resource allocation and resource leveling (El-Sayegh, 2018). However, this time-based planning method is not efficient for repetitive construction projects, as it does not ensure work continuity, does not indicate the location and time where specific crews are assigned, cannot show activity progress levels, does not consider limited resource availability, and fails to provide clear and visual schedules due to redundancies in modeling repeated units (Abdallah & Alshahri, 2018; Amar, 2020; Harris & Ioannou, 1998; Luko, 2009; Mattila & Park, 2003; Yamin & Harmelink, 2001 in Monghasemi & Abdallah, 2021).

On the other hand, the Linear Scheduling Method (LSM) offers advantages such as ease in resource allocation, project progress monitoring and control, and higher efficiency in planning repetitive construction projects. LSM focuses on maximizing labor continuity by allowing workers to perform the same tasks repeatedly at different locations, completing work at one site and immediately moving to the next, thereby minimizing work disruptions (Hyari & El-Rayes, 2006).

However, selecting and applying the appropriate scheduling method in construction projects is not straightforward, as each method has its own strengths and weaknesses. Common scheduling issues include efficient resource allocation, project deadline control, and aligning the characteristics of the scheduling method with project conditions. Project delays can lead to extended completion times, increased costs, and compromised quality and safety (González et al., 2013 in Venkatesh & Venkatesan, 2017). One of the most frequently used methods is the Gantt Chart (Rolfsen & Merschbrock, 2016), but it lacks clarity and efficiency in presentation. Therefore, more specific scheduling methods are needed to address such issues, such as the Linear Scheduling Method (LSM), which emphasizes work flow, or the Precedence Diagramming Method (PDM), which details the logical relationships between activities.

Various analyses of scheduling using LSM and PDM have been conducted in several countries such as the United States (Su & Lucko, 2016), Egypt (Mohamed et al., 2023), and India (Ramani et al., 2022). In Indonesia, similar studies have also been conducted—for example, Mi'raji et al. (2023) compared the effectiveness of LOB and PDM in high-rise building projects and found that LOB was more effective for repetitive work. Another study by Astawa et al. (2020) also supports this, showing that LOB resulted in a faster completion time of 143 days compared to PDM, which took 150 days. However, there is still a gap, as these studies were conducted on small-scale projects and focused solely on duration. These studies form the basis for a more in-depth analysis in this research.

The main objective of this study is to apply LSM in repetitive construction projects and compare it with PDM scheduling for the same project, focusing on labor costs and project duration under two scenarios: normal and accelerated. The DP Mall Expansion building project was selected as a case study, using LSM and PDM as the scheduling methods. The outcomes of both methods were compared in terms of total duration efficiency and labor costs. The results of this study are expected to provide practical recommendations for project managers in selecting the most appropriate scheduling method, thereby enabling more effective labor costs and project durations while minimizing the risk of delays in construction projects.

## LITERATURE REVIEW

In the implementation of a construction project, there are numerous activities involved. The execution of a project requires an appropriate project management system to ensure that the project proceeds according to plan. Project management is the process of planning, scheduling, and controlling a project within a certain period, with a specified cost, desired quality, and in accordance with the available resources (Ammar, 2020). The goal of project management is to manage and coordinate the construction process to achieve optimal results in terms of cost, time, and quality. According to Konior & Szóstak (2020), project management consists of several phases: planning, organizing, implementation, monitoring, and closing. Belferik et al. (2023) state that key characteristics of project management include clear objectives, limited time, constrained resources, risks that must be managed, and the ability to be flexible and adaptive to change.

Scheduling is a key element in construction project management (Nisar & Halim, 2018). Project scheduling is a component of project planning that includes the steps of project control and progress in terms of resource performance—namely cost, labor, equipment, and materials—so that the work can be executed and completed as scheduled (Fahrian et al., 2021). Proper planning allows project activities to begin and end on time, minimizing costs and meeting quality standards. Constraints in project time, cost, or resource availability often lead to inadequate scheduling (García-Nieves et al., 2019). Scheduling typically includes a breakdown of work types, duration of each task, start and finish times, and the interdependencies among tasks. Accelerating the completion time of a project refers to efforts to finish the project earlier than under normal scheduling conditions (I. K. A. A. Putra et al., 2020). The objective of project acceleration is to reduce activity duration. This is done under the assumption that resources are not a constraint, although it will result in increased costs. Duration estimation involves determining the number of work periods required for each activity (Riau et al., 2024).

The **Precedence Diagram Method (PDM)** is a type of network planning scheduling known as Activity on Node (AON). According to Ren & Li (2023), PDM—also referred to as node diagrams or single-arrow network diagrams—is a scheduling technique that uses nodes to represent activities and arrows to indicate logical relationships between them (Srisungnoen & Vatanawood, 2018). In the PDM system, the completion of one activity leads to the start of the next. If the preceding activity is not completed, the subsequent activity cannot begin, which may cause delays in project completion. PDM is considered more flexible than PERT/CPM for large-scale projects (Nisar & Halim, 2018) because it does not require dummy activities. As a result, logical relationships between work items can be created with overlaps without adding more activities (Romadhona et al., 2021).

Duffy et al., as cited in Ramani et al. (2022), explain that the **Linear Scheduling Method (LSM)** is a graphical technique used for time scheduling in projects with repetitive or continuous activities, such as road construction, tunnels, pipeline installations, and others. Linear scheduling is often prepared manually using Microsoft Excel. Other software tools that can be used for LSM include Vito Schedule Planner, TCM Planner, TILOS, DynaRoad, and more (Scala et al., 2023). In LSM scheduling, Microsoft Excel is used to calculate duration, start date, finish date, and buffer time (Salama et al., 2020). According to Chrzanowski and Johnston in Su & Lucko (2016), in LSM, repetitive activities are plotted as lines with constant or variable slopes across two axes—distance/location and time. The placement of these axes depends on the type of project. For linear horizontal projects such as road construction, the horizontal axis represents distance or location, while the vertical axis represents time.

## METHOD

This study employs a quantitative approach with a descriptive-comparative method to compare and analyze project scheduling between the Linear Scheduling Method (LSM) and the Precedence Diagramming Method (PDM). The object of the study is the DP Mall Expansion Project in Semarang, Central Java, conducted from January to July 2024. The variables examined are time and labor costs under both normal and accelerated scheduling scenarios. The research population includes all activities and labor involved in the architectural work of the project. The project was selected as the sample due to its 16 floors and complex activities, making it highly relevant for evaluating the effectiveness of the two scheduling methods.

## RESEARCH RESULTS

According to Su & Lucko (2016), in Linear Scheduling Method (LSM), repetitive activities are plotted as lines with either constant or varying slopes on two axes: distance/location and time. In linear scheduling, Microsoft Excel is used to calculate duration, start date, finish date, and buffer time (Salama et al., 2021). LSM offers several advantages, including the ability to display constraints, productivity rates, and work crew locations (Tang et al., 2018), which helps project managers monitor project workflows more effectively.

To analyze scheduling using the Linear Scheduling Method (LSM), the following steps are involved:

1. Determine the logical relationships between activities
2. Calculate the LSM variables
3. Graph the calculation results
4. Apply delays or accelerations if any preceding work is affected

Work Sequence Logic and Activity Data

The data obtained from the project team is secondary data in the form of an S-curve schedule, which includes types of work and their respective durations. Based on the S-curve, the number of workers needed is calculated using the labor coefficient from the Unit Price Analysis (AHSP) Regulation No. 1 of 2022.

Linear Scheduling Method Variables

1. Calculate the working time for each activity per floor (t)
Example: Basement wall construction

- Duration = 45 days
- Volume = 2246.88 m²
- Daily Productivity = Volume / Duration = 2246.88 / 45 = 49.93 m²/day

2. Estimate the number of work crews for all activity items (H)

- H = 4 crews
  Therefore, across 16 floors, there are four floors for each crew, applying a Finish to Start (FS) relationship among work items with the same crew.

3. Calculate the total number of workers per crew based on each work item (n)
The number of workers for each item varies, as each work item has different durations and crew requirements.

- *n = number of workers per work item*

*Figure 1*

*Linear Scheduling Method Diagram*

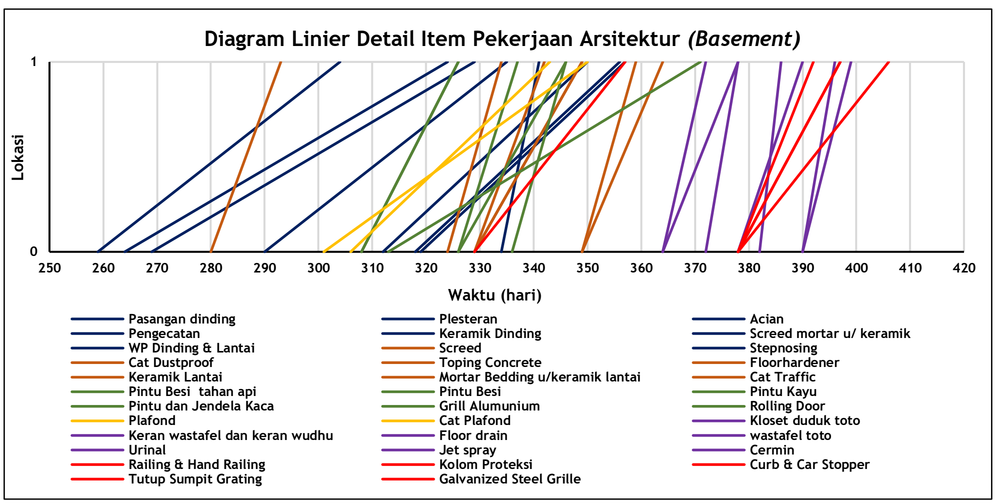


Figure 2 is based on the existing S-curve. The diagram indicates that activities on the basement floor overlap or precede one another. This occurs due to differences in the duration of each task. In Linear Scheduling Method (LSM), the sequence of activities must not intersect—meaning tasks should not disrupt or precede others (predecessors). In other words, the progress of a succeeding activity must not overtake the progress of its predecessor. To address this issue, delay and acceleration trials are carried out by considering the logical relationships between predecessors and successors. For activities at the same location, the logical relationship used is **Start to Start**, whereas for activities at different locations but executed by the same team, the relationship used is **Finish to Start**.

*Figure 2*

*Linear Scheduling Method Diagram with Four Team*

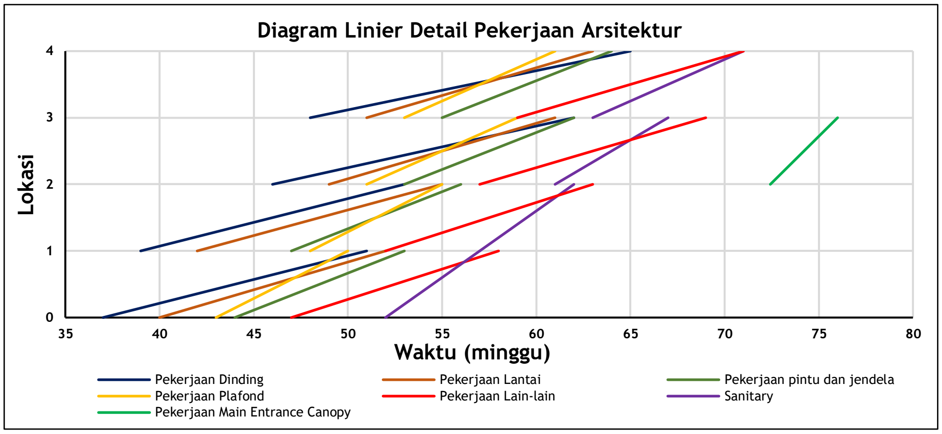


## 4. Delay and Acceleration Trials

Delay and acceleration trials are conducted because some task lines intersect, indicating an absence of clear successor and predecessor relationships. Additionally, these trials are necessary to align the sequence of activities with logical relationships and to avoid conflicts during field implementation.

*Figure 3*

*Linear Scheduling Method Diagram After Delay and Acceleration*

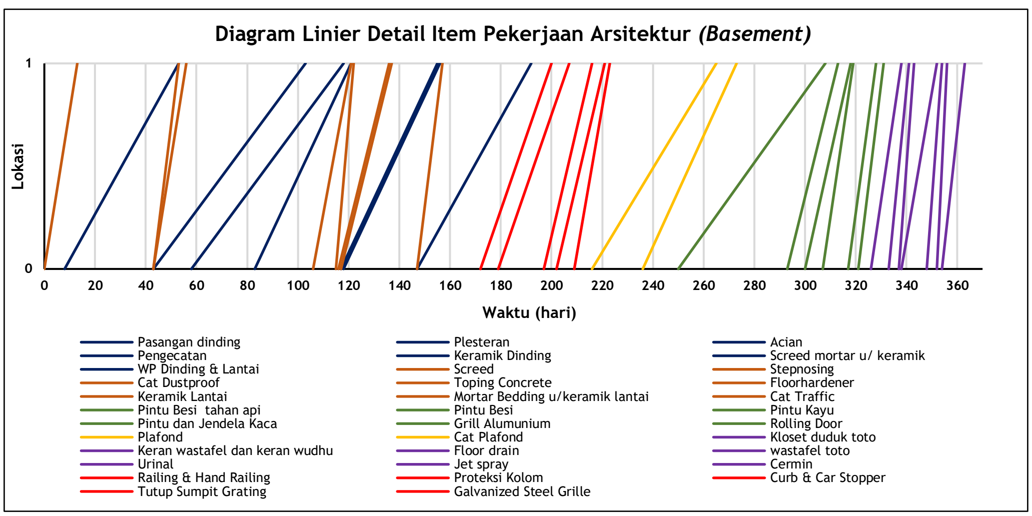


*Figure 4*

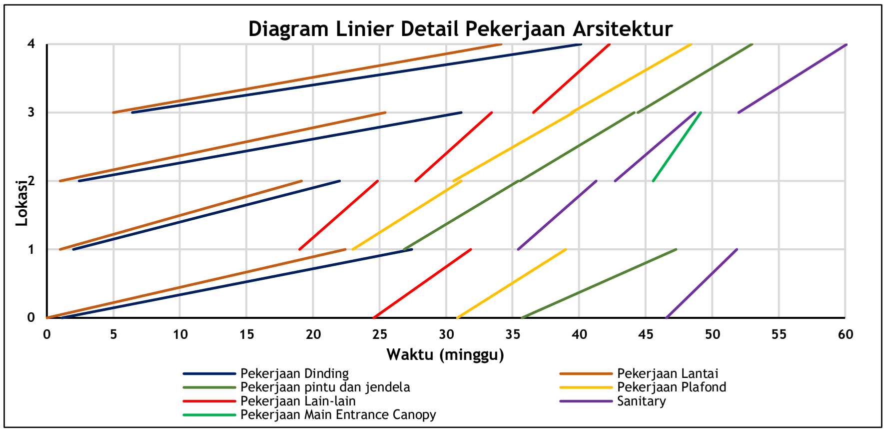


## CONCLUSION

This study employs two different scheduling methods to plan a high-rise building construction project and compares them based on estimated duration and labor wage costs under both normal and accelerated scheduling scenarios. Using the Linear Scheduling Method (LSM), the total duration of architectural work under normal conditions is 877 days, while the accelerated schedule reduces the duration to 284 days—making it 67.61% faster than the normal schedule. Meanwhile, the total duration for the Precedence Diagramming Method (PDM) matches that of the accelerated LSM schedule.

In terms of labor requirements, the LSM under the normal schedule requires 5,803 workers, while the accelerated schedule requires 9,735 workers. Since the LSM and PDM schedules share the same duration under the accelerated scenario, the labor requirements are also identical. The difference in labor requirements leads to a variance in wage costs: the wage cost difference between the normal and accelerated LSM schedules is IDR 6,570,003,519.81. On the other hand, the labor wage cost for both LSM and PDM under the accelerated schedule is the same.

The similarity in results between the LSM and PDM methods is due to the fact that the logical dependency relationships used in PDM can also be applied within LSM, and both methods incorporate buffer time or lag between activities. PDM is effective for identifying the critical path and is well-suited for overlapping tasks; however, it lacks the ability to represent workflow constraints, productivity levels, and clear visualizations—limitations that are addressed by LSM. LSM offers advantages over PDM in terms of visual clarity, productivity tracking, depiction of workflow constraints, and more.

## PENAFIAN

This article aims to provide general information about civil engineering and is not professional advice. The author and publisher are not responsible for any errors, omissions, or repercussions of the use of this information. Always consult with the relevant engineer or expert before implementing the concepts discussed.

## AVAILABILITY OF DATA AND MATERIALS

The data and materials used in this article are obtained from relevant and accountable sources. However, the author does not guarantee the accuracy, completeness, or novelty of the information presented. The use of the data and materials in this article is entirely the responsibility of the reader If required, the reader may contact the author for further information regarding the availability of data and related materials.

## THANKS

Respectfully, I would like to express my deepest gratitude to the UNNES Laboratory of Semarang State University for the guidance, knowledge, and direction provided during the preparation of this article. The support and insights provided are invaluable in understanding and developing the topics discussed, so that they become valuable provisions for me and other colleagues in my academic and professional journey ahead. Again, thank you for all the help and dedication given. I would also like to thank my friends for the support, discussion, and enthusiasm given in completing this article. The togetherness and cooperation that exists is very meaningful in this academic journey.

## REFERENCE


Alafeef, D. M. (2025a). CRITICAL SUCCESS FACTORS FOR SUCCESSFUL CONSTRUCTION PROJECT MANAGEMENT: A COMPREHENSIVE EVALUATION. Journal of Lifestyle and SDG'S Review, 5(2). https://doi.org/10.47172/2965-730X.SDGsReview.v5.n02.pe02802

Alafeef, D. M. (2025b). EVALUATION OF THE CRITICAL SUCCESS FACTORS FOR EFFECTIVE MANAGEMENT OF CONSTRUCTION PROJECTS. Journal of Lifestyle and SDG'S Review, 5(2). https://doi.org/10.47172/2965-730X.SDGsReview.v5.n02.pe02864

Ammar, M. A. (2020). Resource optimisation in line of balance scheduling. Construction Management and Economics, 38(8), 715–725. https://doi.org/10.1080/01446193.2019.1606924

Astawa, I. W. Y., Tastrawati, N. K. T., & Harini, L. P. I. (2020). Waktu Penyelesaian Proyek Konstruksi Menggunakan Precedence Diagram Method dan Line Of Balance. E-Jurnal Matematika, 9(3), 190. https://doi.org/10.24843/mtk.2020.v09.i03.p298

Belferik, R., Andiyan, A., Zulkarnain, I., Munizu, M., Samosir, J. M., Afriyadi, H., Rusmiatmoko, D., Adhicandra, I., Syamil, A., Ichsan, M., & Prasetyo, A. (2023). Manajemen Proyek : Teori & Penerapannya (Efitra & Sepriano, Eds.). PT. Sonpedia Publishing Indonesia.

El-Sayegh, S. (2018). Resource Levelling Optimization Model Considering Float Loss Impact. Engineering, Construction and Architectural Management, 25(5), 639–653. https://doi.org/10.1108/ECAM-10-2016-0229

Fahrian, Haryanto, B., & Jamal, M. (2021). JURNAL TEKNOLOGI SIPIL Jurnal Ilmu Pengetahuan dan teknologi sipil PERBANDINGAN PENJADWALAN PROYEK DENGAN METODE PDM (PRECEDENCE DIAGRAM METHOD) & CPM (CRITICAL PATH METHOD) (Studi Kasus: Lanjutan Pembangunan Proyek Gedung SD Islamic Center Samarinda). Jurnal Teknologi Sipil, 5, 17–25.

García-Nieves, J. D., Ponz-Tienda, J. L., Ospina-Alvarado, A., & Bonilla-Palacios, M. (2019). Multipurpose linear programming optimization model for repetitive activities scheduling in construction projects. Automation in Construction, 105, 1–1. https://doi.org/10.1016/j.autcon.2019.03.020

Hyari, K., & El-Rayes, K. (2006). Optimal Planning and Scheduling for Repetitive Construction Projects. Journal of Management in Engineering, 22(1), 11–19. https://doi.org/10.1061/ASCE0742-597X200622:111

Kementerian Pekerjaan Umum dan Perumahan Rakyat Republik Indonesia. (2022). Peraturan Menteri Pekerjaan Umum dan Perumahan Rakyat Nomor 1 Tahun 2022 tentang Pedoman Penyusunan Perkiraan Biaya Pekerjaan Konstruksi Bidang Pekerjaan Umum dan Perumahan Rakyat. Kementerian Pekerjaan Umum dan Perumahan Rakyat.

Konior, J., & Szóstak, M. (2020). The S-curve as a tool for planning and controlling of construction process-case study. Applied Sciences (Switzerland), 10(6), 1–14. https://doi.org/10.3390/app10062071

Mi'raji, F., Suhana, N., & Komarudin. (2023). Perbandingan Metode Line of Balance dan Precedence Diagram Metod untuk Pekerjaan Konstruksi Gedung 3 Lantai. Jurnal Rekayasa Infrastruktur, 9(2), 118–129.

Monghasemi, S., & Abdallah, M. (2021). Linear Optimization Model to Minimize Total Cost of Repetitive Construction Projects and Identify Order of Units. Journal of Management in Engineering, 37(4). https://doi.org/10.1061/(asce)me.1943-5479.0000936

Muhammad, M. T., Haron, N. A., Alias, A. H., & Harun, A. N. (2017). Strategies to Improve Cost and Time Control using Building Information Model (BIM); Conceptual Paper. Malaysian Construction Research Journal, 1(1), 23–39.

Nisar, J., & Halim, S. (2018). The Effect of Critical Activity on Critical Path and Project Duration in Precedence Diagram Method. International Journal of Structural and Construction Engineering, 12(9), 837–843.

Pemerintah Kota Semarang. (2024). Peraturan Wali Kota Semarang Nomor 3 Tahun 2024 tentang Perubahan Kedua atas Peraturan Wali Kota Semarang Nomor 40 Tahun 2023 tentang Standarisasi Harga

Satuan Bahan Bangunan, Upah, dan Analisa Pekerjaan untuk Kegiatan Pembangunan Pemerintah Kota Semarang Tahun Anggaran 2024. Pemerintah Kota Semarang.

Putra, F. J. (2019). Comparative Analysis of Costs and Time on Scheduling of Project Existing and Linear Method [Skripsi]. Universitas Islam Indonesia.

Putra, I. K. A. A., Indramanik, I. B. G., & Yasa, I. M. S. (2020). PENGARUH PERCEPATAN WAKTU PELAKSANAAN PROYEK KONSTRUKSI GEDUNG TERHADAP BIAYA PELAKSANAAN Studi kasus : Proyek Pembangunan Gedung Lt. III SDN 7 Sesetan. Fakultas Teknik UNR, 12, 40–54.

Ramani, P. V., Selvaraj, P., Shanmugapriya, T., & Gupta, A. (2022). Application of Linear Scheduling in Water Canal Construction with a Comparison of Critical Path Method. Journal of Construction in Developing Countries, 27(1), 189–212. https://doi.org/10.21315/jcdc2022.27.1.11

Ren, Y., & Li, J. (2023). Research on Software Project Schedule Planning Technology Based on the Integration of PERT and CPM. Procedia Computer Science, 228, 253–261. https://doi.org/10.1016/j.procs.2023.11.029

Riau, D. P., Junaidi, J., Akadira, T., Muhtarom, Diana, B. A., & Madya, F. (2024). SOLVING CONSTRUCTION PROJECT DELAYS AS SDGS: EVIDENCE FROM INDONESIA. Journal of Lifestyle and SDG'S Review, 4. https://doi.org/10.47172/2965-730X.SDGsReview.v4.n00.pe01638

Rolfsen, C. N., & Merschbrock, C. (2016). Acceptance of Construction Scheduling Visualizations: Bar-charts, Flowline-charts, or Perhaps BIM? Procedia Engineering, 164, 558–566. https://doi.org/10.1016/j.proeng.2016.11.658

Romadhona, S., Kurniawan, F., & Tistogondo, J. (2021). Project Scheduling Analysis Using the Precedence Diagram Method (PDM) Case Study: Surabaya's City Outer East Ring Road Construction Project (Segment 1). International Journal of Engineering, Science and Information Technology, 1(2), 53–61. https://doi.org/10.52088/ijesty.v1i2.56

Rzepecki, L., & Biruk, S. (2018). Simulation Method for Scheduling Linear Construction Projects Using the Learning-Forgetting Effect. MATEC Web of Conferences, 219, 1–8. https://doi.org/10.1051/matecconf/201821904007

Salama, T., Salah, A., & Moselhi, O. (2021). Integrating Critical Chain Project Management with Last Planner System for Linear Scheduling of Modular Construction. Construction Innovation, 21(4), 525–554.

Scala, N. M., Schiavone, V., Olivieri, H., Seppänen, O., Alves, T. da C. L., Liu, M., & Granja, A. D. (2023). Comparative Analysis of Planning with the Critical Path Method, Last Planner System, and Location-Based Techniques in Brazil, Finland, and the United States. EMJ - Engineering Management Journal, 35(3), 237–256. https://doi.org/10.1080/10429247.2022.2069981

Srisungnoen, W., & Vatanawood, W. (2018). Dependency types validation of precedence diagram method using ontology. Engineering Journal, 22(5), 155–169. https://doi.org/10.4186/ej.2018.22.5.155

Su, Y., & Lucko, G. (2016). Linear Scheduling with Multiple Crews Based on Line-of-Balance and Productivity Scheduling Method with Singularity Functions. Automation in Construction, 70, 38–50. https://doi.org/10.1016/j.autcon.2016.05.011

Tang, Y., Liu, R., & Futian, W. (2018). Scheduling Optimization of Linear Schedule with Constraint Programming. Computer-Aided Civil and Infrastructure Engineering , 33, 124–151. https://doi.org/10.1111/tikus.12277

Tantawy, M. A., Mohammed, S. Z., & Elhakeem, A. (2023). Scheduling of Repetitive Projects Using Line of Balance for Different Scenarios of Activities' Duration Uncertainty. International Journal of Advanced Engineering and Business Sciences, 4(2), 87–99. https://doi.org/10.21608/ijaebs.2023.164910.1046

Utami, A., & Nugraheni, F. (2023). Analisis penjadwalan waktu pelaksanaan proyek dengan Linear Scheduling Method (LSM) pada proyek pembangunan perumahan. Proceeding Civil Engineering Research Forum, 3(1), 72–80.

Venkatesh, P. K., & Venkatesan, V. (2017). Delays in Construction Projects: a Review of Causes, Need and

Scope for Further Research. Malaysian Construction Research Journal, 23(3), 89–103.
Yamín, R. A., & Harmelink, D. J. (2001). Comparison of Linear Scheduling Model (LSM) and Critical Path Method (CPM). Journal of Construction Engineering and Management, 127, 374–381.